AGT

Algebraic & Geometric Topology

Volume 26 (2026)

Mixed-platonic 3-manifolds

Eric Chesebro, Michelle Chu, Jason DeBlois,
Neil R Hoffman, Priyadip Mondal and Genevieve S Walsh

msp

msp

Algebraic & Geometric Topology **26**:6 (2026) 2215–2254
DOI: 10.2140/agt.2026.26.2215
Published: June 22, 2026

Mixed-platonic 3-manifolds

ERIC CHESEBRO, MICHELLE CHU, JASON DEBLOIS,
NEIL R HOFFMAN, PRIYADIP MONDAL AND GENEVIEVE S WALSH

We introduce a class of cusped hyperbolic 3-manifolds that we call mixed-platonic, composed of regular ideal hyperbolic polyhedra of more than one type, which includes certain previously known examples. We establish basic facts about mixed-platonic manifolds which allow us to conclude, among other things, that there is no mixed-platonic hyperbolic knot complement with hidden symmetries.

1 Introduction

Three classical and beautiful hyperbolic knot complements in S^3 are *platonic*, meaning they admit a complete hyperbolic structure that decomposes as a union of isometric copies of a single regular ideal polyhedron. Thurston famously showed that the figure-eight knot complement decomposes into two regular ideal tetrahedra [33, Chapter 3], cf. [34]; and Aitchison and Rubinstein [4] discovered the two "dodecahedral knots", each of whose complement decomposes into two regular ideal dodecahedra. There are many more platonic hyperbolic manifolds — a census is given in [14] — including the complements of the Whitehead link and Borromean rings which were also described in [33, Chapter 3]. However, Hoffman showed that the complements of the figure-eight and the two known dodecahedral knots are the only platonic hyperbolic knot complements in S^3 [18, Corollary 2], building on work of Reid [30] who proved that the only arithmetic hyperbolic knot complement is that of the figure-eight.

The three platonic knot complements are also known to have *hidden symmetries*, meaning that each has an isometry between finite-degree covers that does not descend to the knot complement itself. These are the only hyperbolic knot complements in S^3 known to have hidden symmetries, and in 1995, Neumann and Reid conjectured that they are the only three [21, Problem 3.64(a)]. The conjecture remains open, although many knot complements have been shown not to have hidden symmetries.

Since platonic knots are exactly the knots which are known to admit hidden symmetries, it is natural to investigate the knot complements which are made of at least two types of platonic solids. In this paper we name and initiate a systematic study of *mixed-platonic* manifolds, complete hyperbolic 3-manifolds that decompose into regular ideal polyhedra of more than one type. Section 2 below gives the formal definition and exhibits some examples, including the knot complement $S^3 - 12n706$, that have been known to experts for some time. A certain structural feature of the cusp of $S^3 - 12n706$ might suggest that mixed-platonic knot complements are a promising class to search for more examples with hidden symmetries. However, the main result of this paper shows that this is not so.

MSC2020: primary 57K32; secondary 57K10.
© 2026 MSP (Mathematical Sciences Publishers). Distributed under the Creative Commons Attribution License 4.0 (CC BY).
Open Access made possible by subscribing institutions via Subscribe to Open.

Theorem 6.12 *No mixed-platonic knot complement in S^3 has hidden symmetries.*

The proof of this result, developed over the course of Sections 3 through 6, entails a rich blend of arithmetic, combinatorics, and geometry. Section 3 establishes basic results about mixed-platonic orbifolds, notably the existence of a standard horoball packing (Lemma 3.7) and tight control over the translation length of peripheral elements representing meridians of a mixed-platonic knot complement (Proposition 3.13, proved number-theoretically). Section 4 focuses on *peripheral tilings* of horoball boundaries induced by the polyhedra comprising the decomposition of a mixed-platonic manifold. Every peripheral tiling is a tiling of the plane by equilateral triangles and squares having lattice symmetry. Section 4 gives criteria showing that not every such tiling can be the peripheral tiling of a mixed-platonic orbifold.

The main result of Section 5, Proposition 5.8, classifies the tilings of the plane by equilateral triangles and squares with sidelength 1, having a short translational symmetry and also order-three rotational symmetry. Peripheral tilings of mixed-platonic knot complements with hidden symmetries would have these properties, as recorded in Proposition 5.1. Proposition 5.8 describes three tilings, two of which were shown in Section 4 not to be the peripheral tiling of any one-cusped mixed-platonic manifold. The main result of Section 6, Proposition 6.1, asserts that the full symmetry group of the third tiling — a $(2,3,6)$-rotation group — is not the peripheral subgroup of a mixed-platonic orbifold, and neither is its index-two $(3,3,3)$-rotation subgroup. The proof of Theorem 6.12, which uses the prior results listed above, concludes this section.

While we have shown that the collection of mixed-platonic manifolds does not contain a knot complement with hidden symmetries, our work exhibits numerous nice properties of its members, and it has prompted many further questions. Section 7 lists some of these.

Acknowledgements

This project originated at a SQuaRE which concluded in March 2024 at the American Institute of Mathematics (AIM) in Pasadena, CA. The authors thank AIM for providing a supportive and mathematically rich environment.

Chu was partially supported by NSF grant DMS-2243188, Mondal by Israeli Science Foundation grant 823/23 (through the postdoctoral fellowship at Ben Gurion University), and Walsh by NSF grant DMS-2005353. Mondal also thanks the math department of Rutgers-New Brunswick for providing a supportive work environment during a significant portion of the work.

We thank Matthias Goerner for pointing out an error in our first posted draft, and for other helpful comments. We are also grateful to the referee for comments which have improved the paper's clarity.

2 Definition and existing examples

Definition 2.1 A connected, complete, finite-volume hyperbolic 3-orbifold $M = \mathbb{H}^3/\Gamma$ is *mixed-platonic* if there is a Γ-invariant tiling of $\mathbb{H}^3$ with n_1 Γ-orbits of regular ideal tetrahedra, and n_2 of regular ideal

octahedra, such that $n_1 \geq 1$ and $n_2 \geq 1$. For convenience, the tetrahedra and octahedra in a Γ-invariant decomposition as above are called *tiles*.

This definition is more restrictive than it absolutely has to be, as we now briefly address.

Remark 2.2 We have restricted to finite-volume orbifolds out of convenience (specifically, for counting tiles), since the examples of interest in this paper have finite volume.

Remark 2.3 It is natural to contemplate an a priori broader definition than Definition 2.1, in which regular ideal cubes, dodecahedra, or icosahedra could also occur as tiles. However in such a tiling, a cube (or, respectively, a dodecahedron) could only abut another cube (resp. dodecahedron) along a face, since it is the only platonic solid with quadrilateral (resp. pentagonal) faces. A regular ideal icosahedron does have ideal triangular faces, but it has a dihedral angle of $3\pi/5$ around every edge. For an edge of a putative tiling of $\mathbb{H}^3$ by regular ideal tetrahedra, octahedra, and/or icosahedra, if T, O, and I, respectively, count the number of tetrahedra, octahedra, and icosahedra incident to this edge we must have $(\pi/3)T + (\pi/2)O + (3\pi/5)I = 2\pi$. But all nonnegative integer solutions to this have $I = 0$. Thus like cubes and dodecahedra, icosahedra do not appear as tiles of mixed-platonic manifolds.

Definition 2.4 We call a knot or link in S^3 *mixed-platonic* if its complement admits the structure of a mixed-platonic complete hyperbolic 3-manifold.

Given the constraint $n_1 \geq 1$ and $n_2 \geq 1$, we have that the figure-eight knot complement and the Whitehead link complement are not mixed-platonic. However, there are mixed-platonic manifolds that have been known for some time:

Example 2.5 There are examples of mixed-platonic manifolds described by Maclachlan and Reid in [24, Section 5.6] that are hyperbolic link complements. These are constructed as "hybrids" of the Whitehead link (tiled by ideal octahedra) and a 4-component chain link (tiled by ideal tetrahedra): by cutting along embedded 3-punctured spheres in each (which are necessarily totally geodesic) and gluing the resulting pieces along those 3-punctured spheres. In each original link complement, the three-punctured sphere to be cut along is a union of faces of the link complement's decomposition into regular polyhedra; thus the link complement produced by gluing inherits its polyhedral decomposition from those of the originals.

Example 2.6 Biperiodic alternating links (links embedded in $T^2 \times I$) with mixed-platonic complements were constructed by Champanerkar, Kofman, and Purcell in [6, Theorem 3.5(2)]. This is part of a larger discussion describing link complements, their commensurability, and other invariants via well-understood geometric pieces.

Example 2.7 The complement of the knot pictured on the left in Figure 1 is a mixed-platonic manifold. This knot has the name $12n706$ in the census `HTLinkExteriors` that ships with SnapPy [12]; in particular, it has 12 crossings and is nonalternating. It was studied by D W Boyd and also appears in [15, Section 7.1]. This knot complement decomposes into 6 regular ideal tetrahedra and 2 regular ideal octahedra. An image

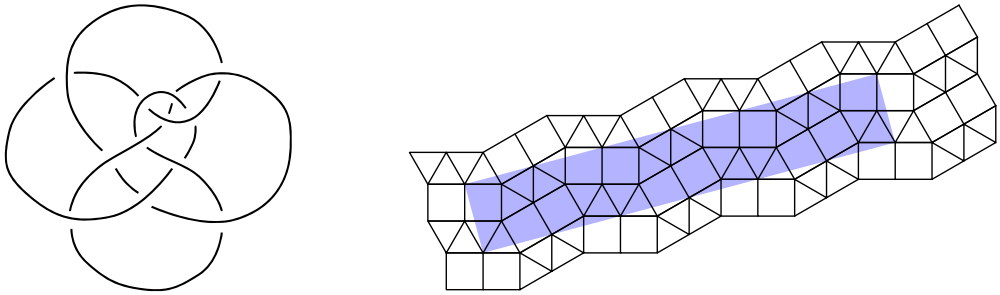

Figure 1: Knot $12n706$ and the peripheral tiling of its complement from SnapPy [12].

of the tiling restricted to the boundary of the horoball at ∞ of height 1 is shown in Figure 1. Here the meridian translates by

$$-\bar{\omega} + i = \frac{-1 + i(\sqrt{3}+2)}{2},$$

a distance of $\sqrt{2+\sqrt{3}}$; compare Proposition 3.13 below.

A notable structural feature of $M_B := S^3 - 12n706$ is visible in the fundamental domain for the knot complement's peripheral subgroup that is outlined in blue on the right-hand side of Figure 1: it is a rectangle with rationally related sidelengths. This implies that its *cusp field* is $\mathbb{Q}(i)$, smaller than the *shape field* generated by the tetrahedral shape parameters determined by its polyhedral decomposition (see [27, Section 2.2] for a discussion of the shape field, denoted there by $k_\Delta\Gamma$).

M_B does not itself have hidden symmetries — this can be seen directly from the fact that the horoball tiling in Figure 1 lacks the requisite rotational symmetries, or as a consequence of [20, Theorem 1.1]. But the fact that its cusp field is smaller than its shape field — a very rare property among census knot complements, and likely a necessary one for the existence of hidden symmetries — suggests that mixed-platonic manifolds are worth further study vis-à-vis hidden symmetries.

Our next example shows that a mixed-platonic manifold can cover a one-cusped, rigid-cusped orbifold. Its features described here can be confirmed directly using SnapPy [12].

Example 2.8 The two-cusped manifold $s913$ in SnapPy's `OrientableCuspedCensus` is mixed-platonic, decomposing as the union of one regular ideal octahedron and two regular ideal tetrahedra. Subdividing the octahedron produces a decomposition of $s913$ into six tetrahedra. It is the only census manifold with eight or fewer tetrahedra that is mixed-platonic: in fact it and $v2774$, which we will discuss further in Example 3.11, are the only such manifolds whose volumes decompose as a positive integer linear combination of those of both the regular ideal tetrahedron and octahedron. We have checked this rigorously, running the verified computations of SnapPy within Sage [32] (script included as an ancillary file in the arXiv posting of this paper [9]).

(Among the nine-tetrahedron census manifolds, at least `o9_44005`, `o9_44006`, `o9_44010`, and `o9_44012` have mixed-platonic decompositions. Interestingly, for each pair of manifolds in this list, there is a four-fold cover common to both indicating that these four manifolds belong to the same commensurability class.)

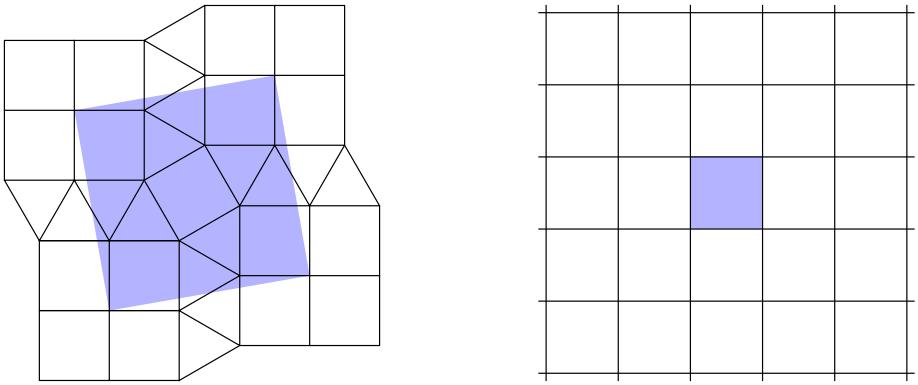

Figure 2: The two cusps of $s913$ induced by a mixed-platonic decomposition. Left: one cusp is tessellated by triangles and squares. Right: the other cusp is tessellated only by squares.

The orientation-preserving symmetry group of $s913$ contains an order-four rotation whose axis of symmetry runs out of a cusp, and another which exchanges the two cusps. Therefore the quotient O' of $s913$ by its orientation-preserving symmetry group is a one-cusped, rigid-cusped orbifold with a $(2,4,4)$ cusp.

As can be seen from horoball cross-sections of the two cusps of $s913$ (see Figure 2), no cusp-exchanging symmetry preserves its decomposition into an octahedron and tetrahedra. Therefore O' does not inherit the structure of a mixed-platonic orbifold from this decomposition of $s913$. Other interesting features of $s913$ are discussed in Example 3.11.

3 Basic results

In the arguments below, it will often be convenient to place the tiling of $\mathbb{H}^3$ by regular ideal tetrahedra and octahedra associated to a mixed-platonic orbifold in a "best" form. This is the *standard position* of our first definition.

Definition 3.1 Using the upper half-space model for $\mathbb{H}^3$, we say that the regular ideal tetrahedron is in *standard position* if its ideal vertices are at 0, 1, ∞ and $\omega = \frac{1}{2}(1+i\sqrt{3})$; and that the regular ideal octahedron is in *standard position* if its ideal vertices are at 0, 1, ∞, $1+i$, i, and $\frac{1}{2}(1+i)$. For a regular ideal tetrahedron or octahedron in standard position, we name its face Δ that has ideal vertices at 0, 1, and ∞.

A tiling of $\mathbb{H}^3$ by regular ideal tetrahedra and/or octahedra is in *standard position* if it has a tile in standard position, and we say that a mixed-platonic orbifold $\mathbb{H}^3/\Gamma$ is *represented in standard position* if Γ leaves invariant a tiling of $\mathbb{H}^3$ by regular ideal tetrahedra and octahedra that is in standard position.

We begin with a lemma that shows that mixed-platonic hyperbolic manifolds and orbifolds are nonarithmetic. This lemma draws out an important feature of the definition of mixed-platonic manifolds in that there are a nonzero number of octahedra and a nonzero number of tetrahedra in any tiling corresponding to a mixed-platonic manifold.

Lemma 3.2 *The invariant trace field of a mixed-platonic hyperbolic 3-manifold is* $\mathbb{Q}(\zeta_{12}) = \mathbb{Q}(\omega, i)$ *where* ζ_{12} *is a primitive 12-th root of unity and* $\omega = \frac{1}{2}(1+\sqrt{-3})$. *In particular, mixed-platonic hyperbolic 3-manifolds are nonarithmetic.*

Before proving this lemma, we point out that a necessary condition for a finite-volume hyperbolic 3-manifold to be arithmetic is that its invariant trace field has exactly one complex place (see [24]). Neumann and Reid show in [27, Theorem 2.4] that the invariant trace field is equal to the number field generated by the shape parameters of a decomposition into ideal tetrahedra, where the shape parameter is defined as in [33, Section 4.1].

Proof Viewing the regular ideal tetrahedron T and octahedron O in standard position, one sees directly that T has shape parameter ω, and that O divides into four isometric ideal tetrahedra sharing an edge with ideal points ∞ and $\frac{1}{2}(1+i)$. One, and therefore all, of these tetrahedra is readily seen to have shape parameter $\frac{1}{2}(1+i)$. A mixed-platonic manifold $M = \mathbb{H}^3/\Gamma$ inherits a decomposition into regular ideal tetrahedra and octahedra projected from the Γ-invariant tiling of $\mathbb{H}^3$; dividing the octahedra further as described above yields a decomposition into ideal tetrahedra with shape parameters ω and $\frac{1}{2}(1+i)$. Since both shapes must be represented in the decomposition, every mixed-platonic manifold has invariant trace field $\mathbb{Q}(i, \omega)$. This field has 2 complex places and hence mixed-platonic manifolds are not arithmetic. □

Note that for an arbitrary mixed-platonic orbifold $\mathbb{H}^3/\Gamma$ with a tiling $\mathcal{P}$ by tetrahedra and octahedra stabilized by Γ, there is an orientation-preserving isometry ϕ such that $\phi(\mathcal{P})$ has a face with vertices at 0, 1, and ∞, and hence $\phi\Gamma\phi^{-1}$ is represented in standard position.

Proposition 3.3 *For any orientable mixed-platonic orbifold* $\mathbb{H}^3/\Gamma$ *represented in standard position,* Γ *belongs to the subgroup of* $\mathrm{PGL}_2(\mathbb{Z}[\zeta_{12}])$ *generated by* $\mathrm{PGL}_2(\mathbb{Z}[\omega])$ *and* $\mathrm{PGL}_2(\mathbb{Z}[i])$. *In particular, each of its elements has determinant in* $\langle\zeta_{12}\rangle$.

Proof Let $\mathcal{P}$ be a Γ-invariant tiling of $\mathbb{H}^3$ by regular ideal tetrahedra and octahedra, in standard position. Below we will follow the common practice of referring to the rings of integers $\mathbb{Z}[\omega]$ and $\mathbb{Z}[i]$ as $\mathbb{O}_3$ and $\mathbb{O}_1$, respectively.

The proof follows by an induction argument from two well-known facts (see, e.g., [17]).

- $\mathrm{PGL}_2(\mathbb{O}_3)$ acts transitively on *flags* of a tiling of $\mathbb{H}^3$ by regular ideal tetrahedra, tuples consisting of a 3-cell of the tiling, one of its faces, an edge of that face, and an ideal endpoint of that edge. The tetrahedron T in standard position belongs to this tiling, so in particular, its stabilizer in $\mathrm{PGL}_2(\mathbb{O}_3)$ acts as the full orientation-preserving combinatorial symmetry group.
- $\mathrm{PGL}_2(\mathbb{O}_1)$ similarly acts transitively on flags of a tiling of $\mathbb{H}^3$ by regular ideal octahedra. The octahedron O in standard position belongs to this tiling, and its stabilizer in $\mathrm{PGL}_2(\mathbb{O}_1)$ acts as the full orientation-preserving combinatorial symmetry group.

Note that both $\mathbb{O}_3$ and $\mathbb{O}_1$ are subrings of $\mathbb{Z}[\zeta_{12}]$, and hence both groups mentioned above are subgroups of $\mathrm{PGL}_2(\mathbb{Z}[\zeta_{12}])$. Moreover, the groups of units of $\mathbb{O}_3$ and $\mathbb{O}_1$ are generated by ω (a primitive sixth root of unity) and i (a primitive fourth root of unity), respectively. Therefore the determinant of a

product of members of $\mathrm{PGL}_2(\mathbb{O}_1)$ and $\mathrm{PGL}_2(\mathbb{O}_3)$ belongs to the smallest multiplicative subgroup of $\mathbb{Z}[\zeta_{12}]$ containing ω and i, which is $\langle\zeta_{12}\rangle$.

For a tetrahedron T (respectively, octahedron O) in standard position in the sense of Definition 3.1, let the *standard T-flag* (resp. *O-flag*) be the tuple $F_T := (T, \Delta, e, \infty)$ (resp. $F_O := (O, \Delta, e, \infty)$), where Δ is the face with ideal vertices 0, 1, and ∞, and e is the edge with endpoints at 0 and ∞. Now take P_0 to be one of T or O in standard position, with matching standard flag F_0. We claim that for any sequence $(F_1, \dots, F_n)$ of flags such that for each i, the three-dimensional polyhedron P_i of F_i is isometric to T or O and intersects P_{i-1} in a face, there exists $\gamma_n = g_n \cdots g_1 g_0$ such that $g_i \in \mathrm{PGL}_2(\mathbb{O}_{j_i})$ for each i, where $j_i = 3$ if P_i is isometric to T and $j_i = 1$ if P_i is isometric to O, taking F_n to F_T or F_O.

The claim is proved by induction on n. For $n = 1$ we can take $\gamma = g_0 g_1$, where $g_0 \in \mathrm{PGL}_2(\mathbb{O}_{j_0})$ stabilizes P_0 and takes the face $P_0 \cap P_1$ to Δ. Then $g_0(P_1)$ has Δ as a face, so it belongs to the $\mathrm{PGL}_2(\mathbb{O}_{j_1})$-invariant tiling by regular ideal tetrahedra or octahedra mentioned in the bullets above. In particular, $g_0(F_1)$ is in the set of flags on which $\mathrm{PGL}_2(\mathbb{O}_{j_1})$ acts transitively. Therefore there is a member g_1 of this group that takes the flag $g_0(F_1)$ to F_T or F_O, and $\gamma_1 = g_1 g_0$ satisfies the conclusion.

Now suppose that $n > 1$ and let $\gamma_{n-1} = g_{n-1} \cdots g_1 g_0$ be the product supplied by the induction hypothesis, taking F_{n-1} to the standard flag matching the type of P_{n-1}. Let g'_{n-1} be an element of $\mathrm{PGL}_2(\mathbb{O}_{j_{n-1}})$ stabilizing $\gamma_{n-1}(P_{n-1})$ (which is one of T or O in standard position) and taking the face $\gamma_{n-1}(P_{n-1} \cap P_n)$ to Δ. Then $g'_{n-1}\gamma_{n-1}(P_n)$ has Δ as a face, so as in the base case there exists $g_n \in \mathrm{PGL}_2(\mathbb{O}_n)$ taking the flag $g'_{n-1}\gamma_{n-1}(F_n)$ to F_T or F_O. Thus,

$$\gamma_n = g_n(g'_{n-1}g_{n-1})g_{n-2} \cdots g_1 g_0$$

is the element required to prove the claim.

We now use the claim to prove the result by fixing a mixed-platonic tiling $\mathcal{P}$ of $\mathbb{H}^3$ in standard position and invariant under the action of a group Γ of isometries, taking F_0 to be the standard flag of the tile P_0 of $\mathcal{P}$ in standard position, and, for a fixed $\gamma \in \Gamma$, taking $F_n = \gamma(F_0)$. Because $\mathcal{P}$ tiles all of $\mathbb{H}^3$, there exists a sequence $(F_1, \dots, F_n)$ of flags satisfying the hypotheses of the claim, such that for each i the three-dimensional polyhedron P_i of F_i is a tile of $\mathcal{P}$. (First find the sequence of tiles $P_1, \dots, P_n$ using connectedness of $\mathcal{P}$, then fill out to flags arbitrarily between F_0 and F_n.) For the isometry γ_n supplied by the claim's conclusion, $\gamma_n\gamma$ fixes the flag F_0, and it follows that $\gamma_n = \gamma^{-1}$. This gives the claimed description of γ. □

Below, a collection $\mathcal{H}$ of horoballs of $\mathbb{H}^3$ is a *packing* if any two distinct members of $\mathcal{H}$ have disjoint interiors. A horoball packing $\mathcal{H}$ is *maximal* if any $B \in \mathcal{H}$ is tangent to at least one other member of $\mathcal{H}$, thus cannot be expanded while keeping $\mathcal{H}$ a packing. It is *invariant under the action of* Γ, a group of isometries, if for every $\gamma \in \Gamma$ and $B \in \mathcal{H}$, $\gamma(B) \in \mathcal{H}$.

Definition 3.4 For a regular ideal tetrahedron or octahedron P, let $\mathcal{H}_P$ be the unique maximal horoball packing by horoballs centered at its ideal vertices that is invariant under the action of the full self-isometry group of P.

Remark 3.5 If P is a regular ideal tetrahedron in standard position as in Definition 3.1 then for each ideal vertex $p \in \{0, 1, \omega\}$, the horoball B_p of $\mathcal{H}_P$ centered at p is the intersection with $\mathbb{H}^3$ of a Euclidean ball of radius $1/2$ that is tangent to $\mathbb{C}$ at p. The horoball B_∞ centered at the final ideal vertex ∞ of P is

$$B_\infty = \{(z, t) \mid z \in \mathbb{C}, t \geq 1\}. \tag{1}$$

One can check this directly, for instance by observing that it is invariant under the order-three rotation fixing ∞ and exchanging the other three vertices, and under the rotation fixing ω and cyclically permuting 0, 1, and ∞.

If P is a regular ideal octahedron in standard position then again B_∞ is as above, and for $p \in \{0, 1, 1+i, i\}$ the horoball B_p is again contained in a Euclidean ball of radius $1/2$ tangent to $\mathbb{C}$ at p. For $p = \frac{1}{2}(1+i)$, B_p is the intersection with $\mathbb{H}^3$ of a Euclidean ball of radius $1/4$ that is tangent to $\mathbb{C}$ at p. This can again be checked directly.

Remark 3.6 It follows from Remark 3.5 that mixed-platonic manifolds can be characterized purely combinatorially as those obtained by gluing ideal tetrahedra and octahedra such that at each edge, either 6 tetrahedra, 4 octahedra, or 3 tetrahedra and 2 octahedra meet. These combinatorics ensure that upon realizing the tetrahedra and octahedra as regular hyperbolic polyhedra and face-pairings as isometries, each point of an edge has a neighborhood isometric to one in $\mathbb{H}^3$; Remark 3.5 guarantees that the resulting hyperbolic manifold is complete.

Lemma 3.7 *Suppose $O = \mathbb{H}^3/\Gamma$ is a mixed-platonic orbifold, and that $\mathcal{P}$ is a Γ-invariant tiling of $\mathbb{H}^3$ by regular ideal octahedra and regular ideal tetrahedra. There is a unique Γ-invariant horoball packing $\mathcal{H}$ of $\mathbb{H}^3$ such that*

(1) *the set of centers of horoballs of $\mathcal{H}$ is the set of ideal vertices of tiles of $\mathcal{P}$; and*

(2) *for each tile P of $\mathcal{P}$ and each ideal vertex p of P, the horoball B_p of $\mathcal{H}$ centered at p belongs to $\mathcal{H}_P$ from Definition 3.4.*

Each such horoball B_p intersects a tile P' of $\mathcal{P}$ if and only if P' has p as an ideal vertex.

If Γ is represented in standard position in the sense of Definition 3.1, in the upper half-space model for $\mathbb{H}^3$, then $\mathcal{H}$ contains a horoball B_∞ centered at ∞ as described in Remark 3.5.

Conversely, $\mathcal{P}$ is the unique tiling by ideal polyhedra with edge set equal to the collection of geodesics joining the centers of tangent horoballs of $\mathcal{H}$ and face set equal to the collection of convex hulls of such geodesics corresponding to triples of pairwise-tangent horoballs of $\mathcal{H}$.

Remark 3.8 We will show in Corollary 6.6 that $\mathcal{P}$ is in fact the *canonical cell decomposition* (aka *Epstein–Penner decomposition*) of $\mathcal{H}$, in the sense established by Epstein and Penner [13].

Proof Conditions (1) and (2) of the statement prescribe that we must have

$$\mathcal{H} = \bigcup_{P \in \mathcal{P}} \mathcal{H}_P,$$

where $\mathcal{H}_P$ is as in Definition 3.4 for each $P \in \mathcal{P}$. Note that if Γ is represented in standard position then some $P \in \mathcal{P}$ is in standard position. So, the horoball B_∞ from Remark 3.5 belongs to $\mathcal{H}_P$. Note also that since $\mathcal{P}$ is Γ-invariant, for any $\gamma \in \Gamma$, γ sends $\mathcal{H}_P$ to $\mathcal{H}_{\gamma(P)}$ for each $P \in \mathcal{P}$. Therefore $\mathcal{H}$ is also Γ-invariant.

We now observe that for any distinct P_0 and P_1 in $\mathcal{P}$ intersecting along a face f, the collections of horoballs belonging to $\mathcal{H}_{P_0}$ and $\mathcal{H}_{P_1}$ and centered at ideal points of f are identical. This is because their intersections with f comprise a set of maximal horodisks invariant under the symmetry group of f, which is an ideal triangle, hence with each disk bounded by a horocyclic arc of length 1. For any distinct P, $P' \in \mathcal{P}$ sharing an ideal point p, there is a sequence $P = P_0, \dots, P_n = P'$ such that P_i shares a face with P_{i-1} for each $i > 0$. The observation above thus implies that for each ideal point p of $\mathcal{P}$, $\mathcal{H}$ has a unique horoball centered at p.

We next claim that for any horoball B of $\mathcal{H}$ centered at an ideal point p of $\mathbb{H}^3$, B intersects only horoballs of $\mathcal{H}$ centered at ideal vertices of tiles of $\mathcal{P}$ with p as an ideal vertex. For any such tile P, the three or four faces of P with p as an ideal vertex (in the respective cases that P is a tetrahedron or octahedron) are each contained in a hyperplane of $\mathbb{H}^3$ that bounds a half-space containing P. B does not intersect any face of P without an ideal vertex at p — this can be checked directly by putting P in standard position with $B = B_\infty$ — so its intersection with the intersection of these three or four half-spaces is equal to its intersection with P. Therefore B is contained in the interior of the union of the tiles of $\mathcal{P}$ having p as an ideal endpoint. The assertion of the final sentence of the lemma's first paragraph follows.

Since this is also true for any other horoball B', B may intersect B' only if there exists $P \in \mathcal{P}$ having both horoballs' centers as ideal vertices, proving the claim.

The fact that each $\mathcal{H}_P$ is a maximal packing now implies that $\mathcal{H}$ is as well. In particular, from the second claim above and the explicit descriptions in Remark 3.5, we find that distinct horoballs B and B' of $\mathcal{H}$ intersect if and only if they are centered at ideal points of an edge of some $P \in \mathcal{P}$; and if so, that they are tangent at a single point of this edge. The edge set of $\mathcal{P}$ is therefore characterized strictly in terms of $\mathcal{H}$ as the set of geodesics joining ideal points of distinct members that have a point of tangency.

We similarly note that each triangular face of $\mathcal{P}$ has a set of three distinct, pairwise-tangent horoballs centered at its ideal points (again this can be seen directly from the descriptions of Remark 3.5). Conversely, for any such triple $\{B_1, B_2, B_3\}$, we claim that the set of centers of the B_i is the set of ideal points of a face of $\mathcal{P}$. To see this, translate B_3 to B_∞, whereupon B_1 and B_2 are taken to Euclidean balls of radius $1/2$ whose centers are at distance 1 due to their tangency. Let e be the edge of $\mathcal{P}$ joining the center p of B_1 to ∞ and let $P_1, \dots, P_k$ be the set of tiles of $\mathcal{P}$ containing e, enumerated in cyclic order so that for each $i > 1$, $P_i \cap P_{i-1}$ is a face f_i containing e, and similarly $P_1 \cap P_k$ is a face f_1. For each such i, f_i has one ideal point at ∞, one at p (the center of B_1), and a third — call it p_i — at distance 1 from p on $\mathbb{C}$. The claim is equivalent to asserting that the center p' of B_2 is one such p_i.

As we observed above, p' is an endpoint of an edge e' of $\mathcal{P}$ with its other endpoint at ∞. The point $e' \cap \partial B_\infty$ is a vertex of a tiling $\mathcal{T}$ of ∂B_∞ by equilateral triangles and squares of sidelength 1 that is obtained by intersecting it with the tiles of $\mathcal{P}$ that have an ideal vertex at ∞. Each vertex of this induced

tiling of $\partial B_\infty = \mathbb{C} \times \{1\}$ lies over an ideal endpoint of an edge of $\mathcal{P}$ with its other endpoint at ∞; in particular, there are vertices over p and each of the p_i described above. For any such i, if $P_i \cap \partial B_\infty$ is a square (i.e., if P_i is an octahedron) then its interior contains the entire open ninety-degree arc of the circle of radius 1 centered at the vertex above p that is bounded by those above p_i and p_{i+1}. If $T := P_i \cap \partial B_\infty$ is a triangle then the corresponding open, sixty-degree circle arc is contained in the interior of the tile of $\mathcal{T}$ that intersects T along its edge containing the vertices over p_i and p_{i+1}. Thus in neither case does the open arc contain any vertex of $\mathcal{T}$, and it follows that the vertices above the p_i are the only ones at distance one from the vertex over p. This implies the claim.

We have showed that the edge set of $\mathcal{P}$ is the collection of geodesics joining the centers of pairs of tangent horoballs of $\mathcal{H}$, and the face set is the collection of ideal triangles determined by triples of pairwise-tangent horoballs. Therefore $\mathcal{P}$ is determined by $\mathcal{H}$, since each of its cells is the closure of a complementary region to the union of the faces. □

For our next result, recall that the *commensurator* of a discrete group of isometries Γ of $\mathbb{H}^3$ is

$$\mathrm{Comm}(\Gamma) = \{\gamma \in \mathrm{Isom}(\mathbb{H}^3) \mid [\Gamma : (\gamma\Gamma\gamma^{-1}) \cap \Gamma] < \infty\};$$

see, e.g., [24, page 269]. Whenever Γ is a nonarithmetic lattice, the commensurator is discrete and is the maximal lattice in the commensurability class of Γ. In this case, the *commensurator quotient* $\mathbb{H}^3/\mathrm{Comm}(\Gamma)$ is the smallest volume orbifold in the commensurability class of $\mathbb{H}^3/\Gamma$ and is covered by all manifolds and orbifolds in the commensurability class. The *orientable commensurator* $\mathrm{Comm}(\Gamma)^+$ and the *orientable commensurator quotient* are defined similarly, restricting to orientation preserving isometries.

Proposition 3.9 *Suppose $M = \mathbb{H}^3/\Gamma$ is a one-cusped mixed-platonic manifold. The commensurator of Γ preserves the Γ-invariant horoball packing $\mathcal{H}$ supplied by Lemma 3.7, hence also the associated Γ-invariant tiling $\mathcal{P}$ by regular ideal tetrahedra and octahedra.*

Proof In this proof it is useful to keep in mind that there is a correspondence between Γ-invariant horoball packings and horospherical cross-sections of $\mathbb{H}^3/\Gamma$: the former project to the latter, and the latter lift to the former, under the universal covering map $\mathbb{H}^3 \to \mathbb{H}^3/\Gamma$.

By Lemma 3.2, M is nonarithmetic. Therefore by Margulis's arithmeticity theorem (see [24, Theorem 10.3.5]), $\mathrm{Comm}(\Gamma)$ is discrete and a finite extension of Γ. We can therefore find a $\mathrm{Comm}(\Gamma)$-invariant horoball packing of $\mathbb{H}^3$, which is thus also Γ-invariant. But since M has only one cusp, there is only one Γ-invariant horoball packing up to Γ-equivariant rescaling (equivalently, any two horospherical cusp cross-sections are rescalings).

It thus follows that $\mathcal{H}$ is a rescaling of the original $\mathrm{Comm}(\Gamma)$-invariant packing and hence is itself $\mathrm{Comm}(\Gamma)$-invariant. The fact that $\mathcal{P}$ is also $\mathrm{Comm}(\Gamma)$-invariant now follows from the final assertion of Lemma 3.7, since it is determined by $\mathcal{H}$. □

Remark 3.10 Thus in this case, $\mathcal{P}$ is the *truly canonical cell decomposition* of Goodman, Heard and Hodgson [15]; cf. Remark 3.8.

Example 3.11 The one-cusped manifold $v2774$ from SnapPy's orientable cusped census shares a double cover with the mixed-platonic manifold $s913$ considered in Example 2.8. Importantly, the Epstein–Penner decomposition for $v2774$ is a *triangulation*,[1] so by Proposition 3.9, $v2774$ is not mixed-platonic. We consider the consequences of this observation for the orientable commensurator quotient O_0 covered by $s913$ and $v2774$. (Note that since $s913$ is mixed-platonic, by Lemma 3.2 it is not arithmetic and the commensurator quotient is an orbifold.) As described by [11], O_0 is the quotient of $\mathbb{H}^3$ by the symmetry group of the horoball packing for $v2274$, which is *not* consistent with the horoball packing for $s913$ associated to the decomposition into regular ideal octahedra and tetrahedra. Therefore O_0 is also not mixed-platonic, since it has a unique horoball packing up to rescaling.

Example 3.11 shows that there are mixed-platonic manifolds that cover orbifolds which are not mixed-platonic, so Proposition 3.9 does not generalize to the multicusped case. Equivalently, per [11], the horoball packing corresponding to a mixed-platonic manifold is not necessarily the maximally symmetric horoball packing.

Example 3.12 Other manifolds in the commensurability class of $v2774$ have interesting properties as well. In fact, a 5-fold, 4-cusped cover of $s913$ given by the triangulation with isomorphism signature ELLvAwzzQvQzAzwPAPPMQcdeffhkjnopmrsqtvrxyvyAzyBCCBDDhsxxfngcwqanxassajarkwankxanjar has two distinct decompositions into tetrahedra and octahedra which can be distinguished by the ratios of their cusp volumes (see [5, Section 3.2] for background on isomorphism signatures). This manifold answers the question of uniqueness, while also showing the importance of the "one-cusped" hypotheses that appear throughout this paper. In order to show the decompositions of this 4-cusped manifold are distinct, we start with an observation that extends Remark 3.6 to computations of cusp volume. Given a mixed-platonic decomposition $\mathcal{P}$, volume of a cusp at an ideal vertex can be computed by $\frac{1}{2}\left(\frac{1}{4}\Delta\sqrt{3}+\square\right)$, where Δ is the number of equilateral triangles in a cellulation of the induced vertex link and $\square$ is a count of the number of squares. To apply this to the two decompositions of this example, we give recipes for two cusp packings that induce two distinct Epstein–Penner decompositions, which are both mixed-platonic decompositions. The first cusp packing is obtained by first inflating cusp neighborhood 0 maximally, then inflating the other cusp neighborhoods until they touch cusp 0. Resulting in a mixed-platonic decomposition determined by the cusp volume ratio of $\left(3\sqrt{3}+\frac{15}{2}:\frac{1}{2}:2:2\sqrt{3}+5\right)$. The second mixed-platonic decomposition is obtained by first maximally inflating cusp 2, then the other cusps until they touch cusp 2, resulting in decomposition determined by a cusp volume ratio of $\left(\frac{3}{2}:\sqrt{3}+\frac{5}{2}:4\sqrt{3}+10:1\right)$. These two ratios of cusp volume are distinct even up to (possible) symmetries of the manifold that exchange the cusps, showing that the underlying mixed-platonic structures are distinct in a meaningful way.

More can be said when further restricting to knot complements among one-cusped manifolds. The following proposition uses the properties of the ring $\mathbb{Z}[\zeta_{12}]$ to control the possible meridians of knot complements in standard position.

[1] This triangulation has isomorphism signature `ovLLwzQAPQcdgejighlkmnmnnmoafaofoqfhahxjo`.

Proposition 3.13 *Suppose $M = \mathbb{H}^3/\Gamma$ is a mixed-platonic knot complement. Any peripheral element of Γ representing a meridian of M has translation length $2+\sqrt{3}$ or $\sqrt{2+\sqrt{3}}$ on the horoball of $\mathcal{H}$ that it stabilizes, where $\mathcal{H}$ is the horoball packing supplied by Lemma 3.7.*

We note that the argument given in our claim below is a version of one in [31, proof of Lemma 3.6] (see also [19, Lemma 3.2]). We include a full proof here for the convenience of the reader.

Proof In the proof we will assume that Γ is represented in standard position, and that the peripheral element in question belongs to the subgroup Λ of Γ stabilizing ∞. It thus has the form $\mu_\infty = \left(\begin{smallmatrix} a & m_\infty \\ 0 & d \end{smallmatrix}\right)$, where a, d, and m_∞ belong to $\mathbb{Z}[\zeta_{12}]$, and $ad \in \langle\zeta_{12}\rangle$, by Proposition 3.3. Since this is a parabolic element of Λ and hence ∞ is its only fixed point on the sphere at infinity, we further have that $a = d$. Thus a is an element of $\mathbb{Z}[\zeta_{12}]$ with $a^2 \in \langle\zeta_{12}\rangle$, and it follows that a itself belongs to $\langle\zeta_{12}\rangle$. Therefore the class of μ_∞ in $\mathrm{PGL}_2(\mathbb{Z}[\zeta_{12}])$ in fact has a matrix representative of the form $\left(\begin{smallmatrix} 1 & m_\infty \\ 0 & 1 \end{smallmatrix}\right)$.

Claim m_∞ is a unit of $\mathbb{Z}[\zeta_{12}]$.

Proof of claim Suppose not; then there is a prime $\mathcal{P}$ of $\mathbb{Z}[\zeta_{12}]$ such that $m_\infty \in \mathcal{P}$. Reducing entries modulo this prime gives a homomorphism from $\mathrm{PGL}_2(\mathbb{Z}[\zeta_{12}])$ to the finite group $\mathrm{PGL}_2(\mathbb{Z}[\zeta_{12}]/\mathcal{P})$ with the meridian μ_∞ in its kernel. Since Γ is normally generated by the meridian μ_∞, it lies entirely in the kernel of this homomorphism if it exists.

However, as Γ is in standard position, there is also a parabolic fixed point at 0, and thus a meridian μ_0 fixing 0 which is conjugate to μ_∞ by an element $g = \left(\begin{smallmatrix} x & y \\ z & w \end{smallmatrix}\right)$ of Γ; that is, with $\mu_\infty = g^{-1}\mu_0 g$. In particular, we must have $g(\infty) = 0$ so $x = 0$. Thus, g cannot represent the identity matrix in $\mathrm{PGL}_2(\mathbb{Z}[\zeta_{12}]/\mathcal{P})$, a contradiction. □

By Lemma 3.7, since Γ is represented in standard position, the horoball B_∞ of $\mathcal{H}$ stabilized by Λ is at height 1. Therefore the translation length of $\left(\begin{smallmatrix} 1 & m_\infty \\ 0 & 1 \end{smallmatrix}\right)$ on ∂B_∞ is the complex modulus $|m_\infty|$ of m_∞. This is the "waist size" of the cusp of M as defined by Adams in [2].

We now appeal to results of [2]. By [2, Lemma 2.4], any cusp of any hyperbolic 3-manifold has waist size at least 1, and [2, Theorem 3.1] asserts that the figure-eight knot complement is the unique hyperbolic 3-manifold having a cusp with waist size equal to 1. Since the figure-eight knot complement is arithmetic, we obtain that $|m_\infty| > 1$ by Lemma 3.2.

Finally, the six theorem [3; 23] implies that $|m_\infty| \leq 6$. We claim that the only units of $\mathbb{Z}[\zeta_{12}]$ with moduli greater than 1 and at most 6 are $\omega + i$, $2+\sqrt{3}$, and their products with powers of ζ_{12}. These have the moduli listed in the proposition statement, so the result will follow from the claim.

For the claim, we first note that $\omega + i$ is a unit, with inverse $1 - i\omega^5$. Since $\mathbb{Q}(\zeta_{12})$ has 2 complex places, the unit group in $\mathbb{Z}[\zeta_{12}]$ is of the form $\mathbb{Z}/12\mathbb{Z}\times\mathbb{Z}$, with the $\mathbb{Z}/12\mathbb{Z}$-factor generated by ζ_{12} and the $\mathbb{Z}$-factor generated by a *fundamental unit* (see [25, Chapter 5] for example). As recorded in [25, page 99], $2+\sqrt{3}$ is the fundamental unit for the real cyclotomic subfield $\mathbb{Q}(\sqrt{3}) \subset \mathbb{Q}(\zeta_{12})$. Thus, as $\mathbb{Q}(\zeta_{12})$ is a degree-two extension of $\mathbb{Q}(\sqrt{3})$, $2+\sqrt{3}$ is either the fundamental unit for $\mathbb{Q}(\zeta_{12})$ or is of the form $u^2\cdot\zeta_{12}^b$, where b is an integer and u is a fundamental unit in the cyclotomic field. It turns out the latter case holds

here, as $\zeta_{12}^7(\omega+i)^2 = (2+\sqrt{3})$, so $\omega+i$ is a fundamental unit for $\mathbb{Z}[\zeta_{12}]$. The claim thus follows by observing that $|\omega+i|^3 > 7$. □

Remark 3.14 As a result of the proof above, we can say more about the off-diagonal entry of a meridian fixing ∞. In particular, m_∞ is a unit of $\mathbb{Z}[\zeta_{12}]$ of the form $\zeta_{12}^k(\omega+i)$ or $\zeta_{12}^k(2+\sqrt{3})$ where ζ_{12} is a primitive 12-th root of unity and $\omega = \frac{1}{2} + \frac{\sqrt{-3}}{2}$.

Proposition 3.15 *Suppose $N = \mathbb{H}^3/\Gamma$ is a mixed-platonic orbifold, let c be a parabolic fixed point of Γ and let Λ be the subgroup of Γ stabilizing c, and let $\mathcal{H}$ be the horoball packing supplied by Lemma 3.7. If Λ has 3-torsion, then the minimal translation length in the horoball H_c based at c in Λ cannot equal $\sqrt{2+\sqrt{3}}$.*

Proof Let $\Lambda_0 \subset \Lambda$ be the maximal abelian subgroup of Λ and assume that Λ_0 is generated by two translations of length ℓ. Then Λ_0 stabilizes a fundamental domain D tessellated by $n_1 > 1$ equilateral triangles and $n_2 > 1$ squares of sidelength 1 in ∂H_c. We stress that since Λ_0 is acting on tessellation of the plane of this form, each translation in Λ_0 translates triangles to triangles and squares to squares. Considering this decomposition, the area is of the form $n_1\frac{\sqrt{3}}{4} + n_2$, where n_1 and n_2 are integers. On the other hand, the area of D is $\frac{1}{2}\ell^2\sqrt{3}$. If $\ell = \sqrt{2+\sqrt{3}}$, then this area is $\sqrt{3}+\frac{3}{2}$. Since $\frac{3}{2} \notin \mathbb{Z}$, there is no valid choice of for n_1 and n_2. □

The following lemma is a summary of [1] with extra details that are relevant to our discussion here.

Lemma 3.16 *Let $N = \mathbb{H}^3/\Gamma$ be a mixed-platonic orbifold with a single rigid cusp. Then the cusp volume of N is at least*

(1) $\sqrt{3}/8$ *if N has an $S^2(2,3,6)$ cusp,*

(2) $\sqrt{3}/4$ *if N has an $S^2(3,3,3)$ cusp, and*

(3) $1/4$ *if N has an $S^2(2,4,4)$ cusp.*

Proof sketch First consider the case that N has an $S^2(2,3,6)$ cusp. Then by [1, Theorem 3.2], if the cusp volume of N is less than $\sqrt{3}/8$, then it is a unique orbifold with cusp volume $\sqrt{3}/24$, $\sqrt{3}/12$, $1/8$, $\sqrt{3}(3+\sqrt{5})/48$, $\sqrt{21}/24$. Orbifolds with the first three cusp volumes are discussed in [28] and noted to be arithmetic. Although not explicitly stated in the Adams' paper, a close reading of his computation shows that if the cusp volume is $\sqrt{3}(3+\sqrt{5})/48$, the orbifold is the tetrahedral orbifold $\Gamma(2,2,5,2,6,3)$ (see [24, Section 4.7.1] for notation), which has invariant trace field $\mathbb{Q}(\sqrt{5},\sqrt{-3})$. The orbifold with cusp volume $\sqrt{21}/24$ is discussed in [19, Lemma 5.1] where a representation of the fundamental group is given. We will use that notation. Using [24, Lemma 3.5.9] with a generating set of $t, r, t.\gamma$, we can compute the invariant trace field from that representation, which is $\mathbb{Q}(\sqrt{-3})$.

Each orbifold with an $S^2(3,3,3)$ cusp on Adams' list in [1, Corollary 4.1] is the unique 2-fold cover of an orbifold with an $S^2(2,3,6)$ cusp and is covered be previous argument.

In the paragraph below [1, Theorem 5.1] and [28], it is discussed that the orbifolds with $S^2(2,4,4)$ and cusp volume 1/8 and $\sqrt{2}/8$ are both arithmetic. □

We conclude this section with a lemma that shows there is only one possible translation length for a meridian of a knot complement that is mixed-platonic and admits hidden symmetries.

Lemma 3.17 *Suppose $M = \mathbb{H}^3/\Gamma$ is a mixed-platonic knot complement with hidden symmetries. Any peripheral element of Γ representing a meridian of M has translation length $2+\sqrt{3}$ on the horoball of $\mathcal{H}$ that it stabilizes, where $\mathcal{H}$ is the horoball packing supplied by Lemma 3.7.*

Proof The assumption that M has hidden symmetries implies that the orientable commensurator quotient $N = \mathbb{H}^3/\operatorname{Comm}^+(\Gamma)$ of M has 3-torsion on the cusp by [20, Theorem 1.1; 27, Proposition 9.1]. Assume that Γ has a meridian of length $\sqrt{2+\sqrt{3}}$. Then the cusp volume for N is at most $\left(\sqrt{2+\sqrt{3}}\right)^2\sqrt{3}/24$ if N has 6-torsion on the cusp and $\left(\sqrt{2+\sqrt{3}}\right)^2\sqrt{3}/12$ if not. Then by Proposition 3.15, we have that the minimal translation length for the peripheral subgroup of $\operatorname{Comm}^+(\Gamma)$ has to be smaller than this. Thus, the cusp volume is at most $\left(\sqrt{2+\sqrt{3}}\right)^2\sqrt{3}/48 < \sqrt{3}/8$ in the 6-torsion case and $\left(\sqrt{2+\sqrt{3}}\right)^2\sqrt{3}/24 < \sqrt{3}/4$ in the other case. In either case, Lemma 3.16 shows that this is not possible. The lemma now follows from Proposition 3.13. □

4 Peripheral tilings

In this section we define *peripheral tilings* of a mixed-platonic manifold or orbifold and prove a series of basic results about them, allowing us to show that certain tilings by triangles and squares cannot be the peripheral tiling of any one-cusped mixed-platonic manifold.

Definition 4.1 A tiling $\mathcal{T}$ of $\mathbb{C}$ is a *peripheral tiling* of a mixed-platonic manifold or orbifold $M = \mathbb{H}^3/\Gamma$ if Γ can be represented in standard position in the sense of Definition 3.1, with Γ-invariant tiling $\mathcal{P}$, such that $\mathcal{T} = \mathcal{P} \cap \partial B_\infty$, where B_∞ is the horoball centered at ∞ of the packing supplied by Lemma 3.7.

Peripheral tilings were considered above (not by name) in Lemma 3.7. As observed there, such a tiling will necessarily be by equilateral triangles and squares, all of sidelength 1.

Lemma 4.2 *For a mixed-platonic orbifold $O = \mathbb{H}^3/\Gamma$ and any fixed cusp c of O, there is a unique peripheral tiling $\mathcal{T}$ of O such that $\mathcal{T} = \mathcal{P} \cap \partial B_\infty$, for B_∞ as in Definition 4.1 projecting to a neighborhood of c.*

Now suppose c is the only cusp of O and, representing Γ in standard position as in Definition 4.1, let Λ be the stabilizer of ∞ in Γ. For $\mathcal{T}$ and B_∞ as above, and for every tile P of $\mathcal{P}$ and every ideal vertex v of P, taking B_v to be the horoball of the packing supplied by Lemma 3.7 that is centered at v, there is a unique Λ-equivalence class of tiles of $\mathcal{T}$ that are Γ-isometric to $P \cap \partial B_v$.

Proof With Γ represented in standard position with associated tiling $\mathcal{P}$, let $\mathcal{H}$ be the horoball packing supplied by Lemma 3.7. Each horoball $B \in \mathcal{H}$ projects to a cusp neighborhood in O, and the preimage of any such cusp cross-section is a Γ-orbit in $\mathcal{H}$. For a fixed cusp c of O and a horoball $B \in \mathcal{H}$ projecting to a neighborhood of c, there is an isometry β of $\mathbb{H}^3$ taking B to B_∞ and putting a tile of $\mathcal{P}$ with an ideal vertex at the center of B into standard position. Thus replacing $\mathcal{P}$ and $\mathcal{H}$ with their images under

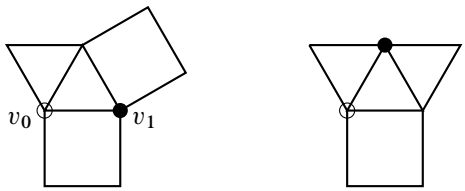

Figure 3: Left: triangular tile of type OOT. Right: triangular tile of type OTT.

this isometry, and Γ by $\delta\Gamma\delta^{-1}$, we have again represented Γ in standard position in such a way that B_∞ projects to c and $\mathcal{T} = \mathcal{P} \cap \partial B_\infty$ is the associated peripheral tiling.

That $\mathcal{T}$ is uniquely associated to c stems from the fact that if δ belongs to Γ then it preserves the tiling $\mathcal{P}$, and hence the replacement procedure above does not change $\mathcal{T}$. And B and B_∞ project to the same cusp of O if and only if they are Γ-equivalent. If O has only one cusp then every horoball of $\mathcal{H}$ is Γ-equivalent to B_∞. In this case, this holds in particular for the horoball $B_v \in \mathcal{H}$ centered at a prescribed ideal vertex v of a prescribed tile P of $\mathcal{P}$, so δ as above takes $P \cap \partial B_v$ to a tile T of $\mathcal{T}$. For another element $\gamma \in \Gamma$ taking B_v to B_∞, $\gamma\delta^{-1} \in \Lambda$ takes T to $\gamma(P \cap \partial B_v)$. □

It is not true that every tiling $\mathcal{T}$ of $\mathbb{C}$ is the peripheral tiling of a mixed-platonic manifold or orbifold. In this section we establish a set of necessary criteria for a tiling to be a peripheral tiling, specifically of a *one-cusped* mixed-platonic manifold or orbifold, and exhibit certain tilings that fail them.

Definition 4.3 For a peripheral tiling $\mathcal{T}$ of a mixed-platonic manifold or orbifold, we declare a triangular tile to be *TTT* if it abuts three triangles of $\mathcal{T}$ along its edges, *OTT* if it abuts a square and two triangles of $\mathcal{T}$, *OOT* if it abuts two squares and a triangle, and *OOO* if it abuts all squares.

Proposition 4.4 *Suppose a tiling $\mathcal{T}$ of $\mathbb{C}$ is a peripheral tiling of a one-cusped, mixed-platonic orbifold. If $\mathcal{T}$ contains triangles of type OOT then it also contains some of type OOO or OTT; and if $\mathcal{T}$ contains some of type OTT then it also contains some of type OOT or TTT.*

Proof Suppose such a tiling $\mathcal{T}$ has triangular tiles of type OOT but none of type OTT. Consider one triangular tile of type OOT as in the left of Figure 3.

Each vertex of $\mathcal{T}$ represents an edge of the associated Γ-invariant tiling of $\mathbb{H}^3$ that has one ideal point at ∞. Let v_0 be the other ideal endpoint of the edge represented by the open-circled vertex in the left of Figure 3, and let P be the regular ideal tetrahedron that intersects $\mathcal{T}$ in the middle triangle (of type OOT). Of the two faces of P containing both v_0 and ∞, one abuts an octahedron and one a tetrahedron. It follows from Lemma 4.2 that there exists $\gamma \in \Gamma$ such that $\gamma(v_0) = \infty$ and $\gamma(P \cap B_{v_0})$ is a tile in $\mathcal{T}$, where B_{v_0} is the horoball of the packing supplied by Lemma 3.7 that is centered at v_0. Now if the final face f of P containing v_0, the one opposite ∞, abuts a tetrahedron, then $\gamma(P \cap B_{v_0})$ is a triangle of type OTT contradicting our assumption. So, f abuts an octahedron. Let v_1 be the ideal vertex at the other endpoint of the edge represented by the shaded-circled vertex. Then all faces of P that contain the ideal vertex v_1 abut octahedra. Thus using Lemma 4.2 again, we can conclude that there is triangular tile of type OOO.

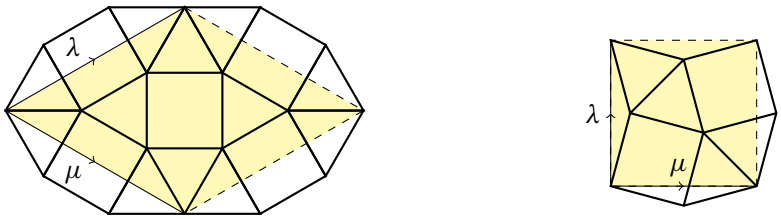

Figure 4: Tilings of $\mathbb{C}$ that cannot appear as peripheral tilings of mixed-platonic manifolds.

An entirely analogous argument using the open circled and the shaded-circled vertices in the right of Figure 3 shows that if $\mathcal{T}$ contains tiles of type OTT and none of type OOT then it also contains some of type TTT. Hence, we are done. □

The result below is a sample application of Proposition 4.4

Corollary 4.5 *Neither tiling of $\mathbb{C}$ consisting of Λ_0-translates of the fundamental domains of Figure 4, where $\Lambda_0 = \langle \mu, \lambda \rangle$, is the peripheral tiling of a one-cusped, mixed-platonic orbifold.*

Proof Inspecting the fundamental domain on the left, we find only triangles of type OOO and OTT. On the right, every triangular tile is of type OOT. Proposition 4.4 now implies the result. □

Lemma 4.6 *For a one-cusped, mixed-platonic manifold $M = \mathbb{H}^3/\Gamma$, upon representing Γ in standard position with $\mathcal{T} \subset \partial B_\infty$, the peripheral subgroup $\Lambda < \Gamma$ stabilizing ∞ has a connected fundamental domain F that is a union of tiles of $\mathcal{T}$, with the property that for every ideal vertex v of every tile P of the associated Γ-invariant tiling of $\mathbb{H}^3$, there is a unique $\gamma \in \Gamma$ taking v to ∞ such that $\gamma.P \cap \mathcal{T}$ is a tile of F. In particular, F has exactly $4n_1$ triangular faces, and $6n_2$ octahedral faces, for n_1 and n_2 as in Definition 2.1.*

Proof The key observation here is that if $M = \mathbb{H}^3/\Gamma$ is a one-cusped hyperbolic 3-orbifold, then any two horoballs of the packing $\mathcal{H}$ supplied by Lemma 3.7 are Γ-equivalent. By the definition of mixed-platonic orbifolds, the Γ-invariant tiling by tetrahedra and octahedra has at least one Γ-orbit of each type. Any ideal tetrahedron of this tiling has a horoball of $\mathcal{H}$ centered at each of its ideal points; hence a Γ-translate of this tetrahedron has an ideal vertex at ∞ — and therefore intersects ∂B_∞. The same holds for ideal octahedra.

Restricting now to the case that M is a manifold, then Γ is torsion-free and no element of the peripheral subgroup Λ stabilizing $\mathcal{T}$ takes any square or triangle to itself. It is thus possible to construct a fundamental domain for Λ as a union of squares and triangles, by starting with a given tile and working outward along edges, including each newly encountered tile in the union if and only if its Λ-orbit does not belong to the union. This process terminates, since $\partial B_\infty/\Lambda$ has finite area. It yields a connected union F of squares and triangles, containing at most one representative of each Λ-orbit, with the property that each tile edge in the frontier of F is the intersection of a tile in F and a tile outside F that is Λ-equivalent to one inside of it. We claim that F contains a representative of *every* Λ-orbit and hence is the desired fundamental domain.

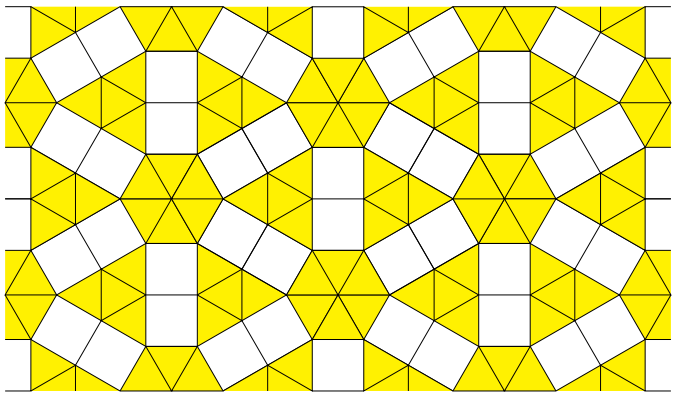

Figure 5: $\mathcal{R}$: a tiling of the plane where each square is surrounded by three triangles and one other square, which also has symmetries of order 3.

If this were not the case then by choosing a tile P of $\mathcal{T}$ that is closest to F with the property that its orbit is not represented in F, we can ensure that a tile P' abutting P does have its Λ-orbit represented in F. But then the element of Λ that moves P' into F would take P either into or adjacent to F, respectively contradicting either the selection of P or the construction of F. This proves the claim.

In the case that M is a manifold and hence Γ is torsion-free, we note further that no element of Γ stabilizes any tile of its invariant tiling. Since M is one-cusped it follows that each Γ-orbit of tetrahedra (resp. octahedra) yields exactly four (resp. six) distinct Λ-orbits of triangles (resp. quadrilaterals) in $\mathcal{T}$. □

We conclude this section by using a more sophisticated version of the same approach to prove the following result, addressing a tiling that proves exceptional from other perspectives.

Proposition 4.7 *The tiling $\mathcal{R}$ pictured in Figure 5 is not the peripheral tiling of a one-cusped mixed-platonic manifold.*

Proof The orientation-preserving symmetry group Λ_0 of $\mathcal{R}$ has an order-six rotation fixing the center of each hexagonal region that is a union of triangles of $\mathcal{R}$ (yellow in the figure); an order-three rotation fixing the center of each triangular region that is a union of triangles of $\mathcal{R}$ (also yellow in the figure), and an order-two rotation exchanging any pair of squares of $\mathcal{R}$ that share an edge. Therefore it is a $(2,3,6)$-rotation group. It acts on the triangle classes as follows:

- transitively on TTT triangles — each of which is at the center of a yellow triangular region, and has a stabilizer of order three;
- simply transitively on the OTT triangles, which occupy the yellow hexagonal regions;
- simply transitively on the OOT triangles, each of which lies in a corner of a yellow triangular region; and
- simply transitively on squares.

Consequentially, a fundamental domain for Λ_0 must contain the area of one square, OTT triangle, and OOT triangle each, and one-third the area of a TTT triangle. Therefore any lattice subgroup Λ of Λ_0 that

has d distinct orbits of squares will also have d distinct orbits each of OOT and OTT triangles, and $d/3$ distinct orbits of TTT triangles.

Now let us suppose that a one-cusped mixed-platonic manifold M that divides into regular ideal tetrahedra and octahedra has the tiling of $\mathcal{R}$ as its peripheral tiling. We classify the tetrahedra decomposing M as follows:

- "TTTT", for those abutting tetrahedra across all faces;
- "OOTT", for those abutting octahedra across two faces and tetrahedra across the others; and
- "OTTT", for those abutting an octahedron across one face and tetrahedra across the others.

Of the four triangular horospherical cross sections of the ideal vertices of a tetrahedron, for the types above we have the following classification:

- for a tetrahedron of type TTTT, all four triangles are of type TTT;
- for a tetrahedron of type OOTT, two triangles are of type OTT, and two are of type OOT;
- for a tetrahedron of type OTTT, three triangles are of type OTT, and one is of type TTT.

Note that while there could in principle be other tetrahedron types (e.g., OOOT), these all have at least one vertex with a triangular horospherical cross section not represented in $\mathcal{R}$. So the decomposition of M must only involve tetrahedra of types TTTT, OOTT and OTTT. We take the numbers of these to be a, b and c, respectively.

Now suppose the decomposition of M has σ distinct octahedra. Since each octahedron has six ideal vertices, each with horospherical cross section a square, the peripheral tiling of M has $d = 6\sigma$ squares. We thus find that:

- $d = 2b + 3c$, counting triangles of type OTT;
- $d = 2b$, counting triangles of type OOT; and
- $d = 3(4a + c)$, counting triangles of type TTT.

The first two equations give that $c = 0$, whereupon we further obtain $a = d/12 = \sigma/2$ and $b = d/2 = 3\sigma$. In particular, σ must be even.

But the only takeaway that we will use here is that every triangle of type OTT comes from a tetrahedron of type OOTT, since there are no tetrahedra of type OTTT ("$c = 0$" above). Consider a hexagon H from the tiling of Figure 5, the union of six OTT triangles sharing a vertex. Each such triangle is the ideal vertex of an OOTT tetrahedron. For adjacent such tetrahedra T_1 and T_2, let f be the triangular face that they share and let v be the ideal vertex of f that does not belong to the edge of f with one endpoint at the rotation center of H. Let B_v be the horoball of the packing from Lemma 3.7 that is centered at v.

For each of $i = 1, 2$, the horospherical cross section $B_v \cap T_i$ is a triangle of type OOT in B_v, and the two cross-sectional triangles $B_v \cap T_1$ and $B_v \cap T_2$ meet each other across their "T" edges. But no such arrangement occurs in the tiling of Figure 5, where each OOT triangle intersects a TTT triangle across its

"T" edge. This contradicts the hypothesis that M is one-cusped, since every cross-sectional triangle of every polyhedron in its decomposition must lift to a tile of the figure. □

5 Classifying rotationally symmetric tilings with a short translation

In this section, we classify tilings of $\mathbb{R}^2$ that satisfy the necessary conditions listed below for being the peripheral tiling of a mixed-platonic knot complement with hidden symmetries.

Proposition 5.1 *The peripheral tiling of a mixed-platonic knot complement with hidden symmetries is a tiling of $\mathbb{R}^2$ by unit-sidelength squares and equilateral triangles possessing both order-3 rotational symmetry and a translational symmetry of length at most $2+\sqrt{3}$.*

Proof Suppose $M = \mathbb{H}^3/\Gamma$ is a mixed-platonic knot complement with hidden symmetries. Since M is mixed-platonic it is nonarithmetic, by Lemma 3.2, so the commensurator $\mathrm{Comm}(\Gamma)$ is discrete. By Lemma 3.7, the Γ-invariant tiling $\mathcal{P}$ by regular ideal tetrahedra and octahedra is also $\mathrm{Comm}(\Gamma)$-invariant. Let $\mathrm{Comm}^+(\Gamma)$ be the orientation-preserving subgroup of $\mathrm{Comm}(\Gamma)$. The orientable commensurator quotient $O := \mathbb{H}^3/\mathrm{Comm}^+(\Gamma)$ is then itself mixed-platonic.

Since M has hidden symmetries, O has a rigid cusp by [27, Proposition 9.1]. It then follows from [20, Theorem 1.1] and the classification of Euclidean orbifolds that O has either a $(2,3,6)$- or $(3,3,3)$-cusp. With O represented in standard position as in Definition 3.1, let $\mathcal{T}$ be the peripheral tiling (of both M and O) from Definition 4.1, contained in the horoball B_∞ centered at ∞ of the horoball packing from Lemma 3.7. As discussed in Section 4, $\mathcal{T}$ is a tiling of $\mathbb{R}^2$ by unit-length equilateral triangles (the intersections with B_∞ of the tetrahedra of $\mathcal{P}$) and squares (from octahedra of $\mathcal{P}$).

Let Λ be the peripheral subgroup of $\mathrm{Comm}^+(\Gamma)$ stabilizing B_∞. Then Λ has order-three rotations, being a $(2,3,6)$- or $(3,3,3)$-rotation group, and it leaves $\mathcal{T}$ invariant. Let $\Lambda_0 < \Lambda$ be the peripheral subgroup of Γ stabilizing B_∞. By Proposition 3.13, the element of Λ_0 representing a meridian acts on ∂B_∞ as a translation by at most $2+\sqrt{3}$; hence this is an upper bound for the minimum translation length of infinite-order elements of Λ. □

The section's main result, Proposition 5.8, asserts that there are three of these, generated from fundamental domains in Figure 9 as described in Remark 5.7. We call them $\mathcal{Q}$ (which is also pictured on the left in Figure 4), $\mathcal{R}$ (also in Figure 5), and $\mathcal{S}$ (also in Figure 12). While the results here follow from classifications of more general plane tilings, we include a complete proof in the interests of keeping the paper self-contained.

We first briefly relate our results to the general classification of plane tilings with a cocompact symmetry group. Such tilings are usually called *k-uniform* and classified by k, defined to be the number of transitivity classes (i.e., orbits) of vertices under the action of the full symmetry group of the tiling. A close reading of our arguments below does lead to the conclusion that the tilings we are interested in appear in the list of k-uniform tilings for $k=2$ or $k=3$. The tiling $\mathcal{Q}$ is one of the twenty 2-uniform tilings of the plane, and $\mathcal{R}$ and $\mathcal{S}$ are each among the sixty-one 3-uniform tilings of the plane (see [22] for a classification

of 2-uniform tilings, [7; 8] for a classification and relevant discussion of 3-uniform tilings, and [16] for further background). In particular, these classifications often contain tilings that allow for tiles with more than four sides (e.g., hexagons and 12-gons). Just as relevant, to apply those results we would also need to show that the full symmetry groups contain both order-6 rotations and reflections. While these conclusions can be inferred from the classification contained here, we present the argument this way because it more directly connects notations of translation length to an enumeration of valid peripheral tilings.

It also follows from this section that the tilings of the plane by equilateral triangles and squares with a rotation of order 3 and shortest translation length *equal to* $2+\sqrt{3}$ are exactly $\mathcal{R}$ (see Figure 5) and $\mathcal{S}$ (see Figure 12). Alternative names for $\mathcal{R}$ include $[3^6; 3^3 4^2; 3^2 4.3.4]$. This notation classifies the cyclic orders of polygons incident to the three orbits of vertices: in this case, one vertex is incident to six triangles; a second, to three successive triangles followed by two squares; and the third to two triangles, one square, and a third triangle before being capped off by a final square. The notation for $\mathcal{S}$ is $[3^6; 3^2 4.3.4; 3^2 4.3.4]$.

The rest of the section leads up to the proof of Proposition 5.8.

Lemma 5.2 *Fix $t>0$ and suppose Λ is a discrete, cocompact group of orientation-preserving isometries of $\mathbb{R}^2$ containing rotations of order three, such that the minimal translation length of any infinite-order element of Λ is t. Then:*

- *There is a tiling of $\mathbb{R}^2$ by equilateral triangles with sides of length $t/\sqrt{3}$, whose vertex set is the set of fixed points of order-three rotations in Λ. For any triangle Δ of this tiling every conjugacy class of order-three elements of Λ has a representative fixing a vertex of Δ.*
- *Every point of $\mathbb{R}^2$ is within a distance of $t/3$ from a fixed point of an order-three rotation belonging to Λ.*

Proof This is a consequence of the well-known classification of groups of Euclidean isometries. First, any group Λ satisfying the hypotheses is either a $(2,3,6)$- or $(3,3,3)$-rotation group. In the latter case, this means that there is a Λ-invariant tiling of $\mathbb{R}^2$ by equilateral triangles, with a fundamental domain for the Λ-action that is the union of two adjacent tiles, such that Λ is generated by order-three rotations fixing the endpoints of the shared edge. Taking a and b to be distinct, counterclockwise such rotations, their product ab fixes the third vertex of one of the two fundamental domain tiles and represents the final conjugacy class of order-three elements of Λ.

The fourth fundamental domain vertex is fixed by ba, which is conjugate to ab. For every triangle of the Λ-invariant tiling, it follows that its three vertices are fixed by order-three rotations representing the three distinct conjugacy classes in Λ. Any $\lambda\in\Lambda$ carries the fixed point of a rotation $\rho\in\Lambda$ to the fixed point of $\lambda\rho\lambda^{-1}$. It follows that if λ is a translation, its translation length must be at least the minimum distance between fixed points of rotations belonging to the same conjugacy class. If the tiles have side length x, this distance equals $x\sqrt{3}$, which is the distance between the fixed points of ab and ba. Note that the lower bound is realized by the translation bab.

This implies the lemma's conclusion (1) in the case that Λ is a $(3,3,3)$-rotation group. Conclusion (2) follows by observing that in an equilateral triangle with sides of length x, the point at maximum distance

from the set of vertices is the triangle's centroid, which is at distance $x/\sqrt{3}$ from each of them. Thus if $x = t/\sqrt{3}$, this distance is $t/3$, and the lemma is proved in the case that Λ is a $(3,3,3)$-rotation group.

In the case that Λ is a $(2,3,6)$-rotation group, it has a unique index-two subgroup Λ_0, which is a $(3,3,3)$-rotation group. In this case, Λ also leaves invariant the Λ_0-invariant tiling described above, and there is a choice of two-tile fundamental domain F_0 for Λ_0 such that Λ is generated by an order-three rotation fixing the shared edge and an order-two rotation acting on it by reflection. Dividing F_0 in half by a perpendicular bisector of this edge thus yields a fundamental domain for Λ. Calling the order-three rotation a and the order-two rotation c, we have that b from before equals cac, and ac is an order-six rotation with the same fixed point as $ab = (ac)^2$. It follows that the order-three fixed points of Λ are those of Λ_0, and conclusions (1) and (2) follow from the previous case. □

Lemma 5.3 *If a tiling $\mathcal{T}$ of $\mathbb{C}$ into squares and equilateral triangles of sidelength 1 has an order 3 rotational symmetry r, then the fixed point of r is either the centroid of a triangle in $\mathcal{T}$ or a vertex of a triangle in $\mathcal{T}$ that is not incident to any square of $\mathcal{T}$. In the latter case, six triangles of $\mathcal{T}$ meet at this vertex.*

Proof Let p be the center of an order 3 rotation r of $\mathcal{T}$. Then p is either a vertex of $\mathcal{T}$ or lies inside in the interior of an edge of $\mathcal{T}$ or lies inside the interior of a tile of $\mathcal{T}$.

Now, p cannot lie inside the interior of an edge of $\mathcal{T}$ by consideration of the two endpoints, since a rotation of order 3 acting on $\mathbb{R}^2$ cannot stabilize an edge.

If p lies inside the interior of a tile then r would have to send that tile to itself by acting as a 3-cycle on its vertices. This would mean that the tile cannot be a square tile as otherwise it would contradict that its fixed point p is in the interior. When the tile is triangular, r would have to fix its centroid implying p is the centroid.

If p is a vertex of $\mathcal{T}$, r cannot fix any tile that contains p as a vertex. But, if p is incident to a square tile, then r would act as a 3-cycle on the square tiles that contain p as a vertex. This forces p to be incident to only square tiles and as a consequence r will have to fix a square tile incident to p, a contradiction.

So, this shows that p is either the centroid of a triangular tile or a vertex of $\mathcal{T}$ that is not incident to any square tile. In the latter case, p is then necessarily the shared vertex of six triangular tiles of $\mathcal{T}$. □

Lemma 5.4 *Suppose Λ is a discrete, cocompact group of orientation-preserving isometries of $\mathbb{R}^2$ containing rotations of order three that leaves invariant a tiling $\mathcal{T}$ of $\mathbb{C}$ into squares and equilateral triangles of sidelength 1, and such that the minimal translation length of any infinite-order element of Λ is at most $2+\sqrt{3}$. For a square tile of $\mathcal{T}$, referring to its center (i.e., the point equidistant from its vertices) as c, let p be a nearest fixed point to c of an order-three rotation belonging to Λ. The union of the tiles of $\mathcal{T}$ that intersect the line segment joining p to c is isometric to one of the two configurations of Figure 6.*

Proof By Lemma 5.2, the distance from c to p is at most $(2+\sqrt{3})/3 < 1.245$. By Lemma 5.3, p is either the centroid of a triangle of $\mathcal{T}$ or the shared vertex of six triangles of $\mathcal{T}$. For an equilateral triangle with sidelength 1, the shortest distance from a vertex to the side opposite it is $\sqrt{3}/2$. It follows that if p is the shared vertex of six equilateral triangles then there is an open disk of radius $\sqrt{3}/2$ centered at p

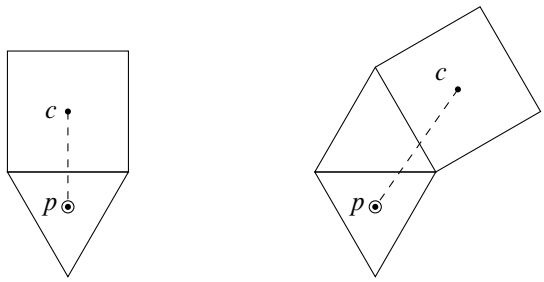

Figure 6: Possible nearest rotation fixed points to square centers.

and contained in their union. Since there is an open disk of radius $1/2$ centered at c and contained in the interior of the square tile containing it, the distance from p to c would be at least $1/2+\sqrt{3}/2>1.366$ in this case. But this is larger than $(2+\sqrt{3})/3$.

Therefore p is the centroid of a triangle T of $\mathcal{T}$. If the square tile containing c is adjacent to T then the union of tiles intersecting the line segment $[p,c]$ from p to c is as pictured on the left in Figure 6. So let us assume that this is not the case, and let T_1 be a tile of $\mathcal{T}$ adjacent to T and intersecting $[p,c]$. We claim first that T_1 is not a square.

Supposing that T_1 is a square, we observe first that neither tile of $\mathcal{T}$ that intersects T_1 along an edge that shares a single vertex with $T_1\cap T$ is a square, since this is not compatible with the existence of an order-three rotation fixing T and preserving $\mathcal{T}$. Therefore both such tiles are triangles, and the union of T, T_1, and these two is pictured on the left in Figure 7.

Since the line segment $[p,c]$ intersects the edge $T\cap T_1$, it exits the pictured union of triangles and squares within the cone defined by the dashed lines in the figure. However, the minimum distance from p to the union of edges in the boundary of this region is $1+1/(2\sqrt{3})>1.288$, realized by the arc joining p to the midpoint of the edge of T_1 opposite $T_1\cap T$. This is already larger than $(2+\sqrt{3})/3$, a contradiction that proves the claim.

Recall that the claim asserted that if T_1 does not contain c then it is a triangle. We now assume this is the case and let $T_2\neq T_1$ be the tile of $\mathcal{T}$ other than T that shares an edge with T_1 and intersects $[p,c]$. Let v be the vertex of T at which $T\cap T_1$ and $T_1\cap T_2$ meet. If T_2 were a triangle then by the rotation-invariance of T, v would be contained in at least four — hence exactly six — triangles. Then $[p,c]$ would exit the union of the triangles containing v in either T_2 or the unlabeled triangle on the

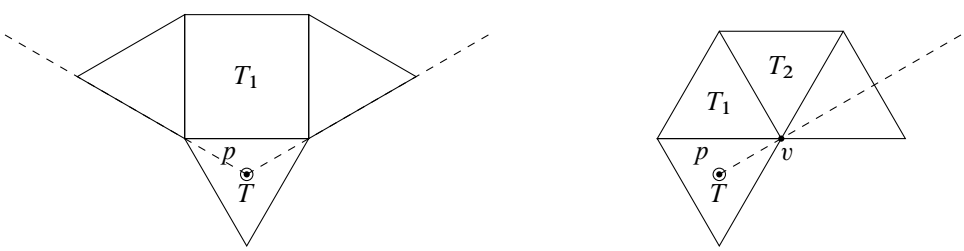

Figure 7: Two forbidden configurations.

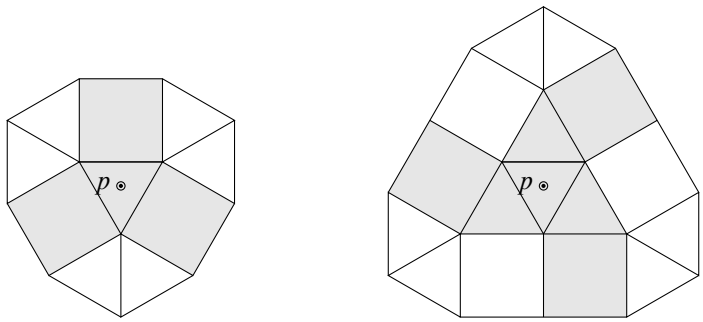

Figure 8: Rotation-invariant square carriers.

right in Figure 7. The distance from p to the closest point of the edge of either of these triangles is $\sqrt{3}/2+1/(2\sqrt{3})>1.154$. The length of $[p,c]$ is at least $1/2$ larger than this, since this is a lower bound on the length of its intersection with the square tile containing c. Since this is larger than $(2+\sqrt{3})/3$, T_2 cannot be a triangle.

Therefore in the case that T_1 does not contain c, it is a triangle and $T_2\neq T$ — the tile of $\mathcal{T}$ that shares an edge with T_1 and intersects $[p,c]$ — is a square. By arguing as in the case of the paragraph above we can show that if c were not the center of T_2 then $[p,c]$ would be too long; so c is the center of T_2 and, up to isometry, the configuration $T\cup T_1\cup T_2$ is as pictured on the right in Figure 6. □

Corollary 5.5 *Suppose Λ is a discrete, cocompact group of orientation-preserving isometries of $\mathbb{R}^2$ containing rotations of order three that leaves invariant a tiling $\mathcal{T}$ of $\mathbb{C}$ into squares and equilateral triangles of side length 1, and such that the minimal translation length of any infinite-order element of Λ is at most $2+\sqrt{3}$. Every square tile of $\mathcal{T}$ is contained in a region isometric to one of the two pictured in Figure 8, with a fixed point of a rotation of Λ at its center.*

Proof Fix a square tile S of $\mathcal{T}$, and call its center c. By Lemma 5.4, up to isometry S is the square tile in one of the two configurations pictured in Figure 6, where p is a nearest fixed point to c of an order-three rotation $\lambda\in\Lambda$. The union of this configuration with its images under λ and λ^{-1} is one of the two shaded regions in Figure 8. The remainder of each neighborhood in the figure is then determined by the shaded region and the geometry of the two tile types in $\mathcal{T}$. □

Notation For the rest of this section, we will refer to the neighborhoods pictured in Figure 8 as *Rotation-Invariant Square Carriers*, or *RISC*s for short.

Lemma 5.6 *Suppose Λ is a discrete, cocompact group of orientation-preserving isometries of $\mathbb{R}^2$ containing rotations of order three that leaves invariant a tiling $\mathcal{T}$ of $\mathbb{C}$ into squares and equilateral triangles of sidelength 1 — with each shape represented — such that the minimal translation length of any infinite-order element of Λ is at most $2+\sqrt{3}$. If $\mathcal{T}$ contains a pair of distinct RISC neighborhoods with rotation centers at a distance less than $\ell=2+1/\sqrt{3}$, then the union of these two neighborhoods forms one of the three configurations of Figure 9.*

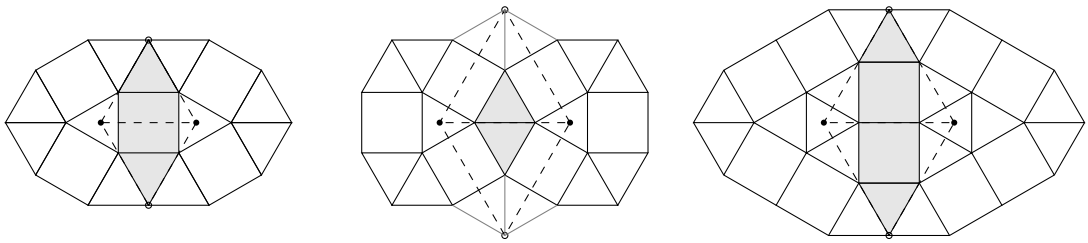

Figure 9: Unions of RISC neighborhoods with centers at distance $\leq 2+\sqrt{3}$; overlap shaded. Additional gray triangles in the middle figure belong to any tiling by equilateral triangles and squares which contains that configuration. The group generated by order-three rotations fixing the two RISC centers extends the pictured tilings to tilings of $\mathbb{R}^2$ that we respectively call $\mathcal{Q}$ (also pictured in Figure 4), $\mathcal{S}$ (also in Figure 12) and $\mathcal{R}$ (also in Figure 5).

Remark 5.7 In each case of the figure, the union of the two dashed equilateral triangles forms a fundamental domain for the subgroup of Λ generated by the order-three rotations at the RISC rotation centers. Hence $\mathcal{T}$ is determined in each case by its intersection with this fundamental domain.

Proof of Lemma 5.6 A Euclidean geometry computation shows that the left-hand RISC neighborhood of Figure 8 contains an open disk of radius $1+1/(2\sqrt{3}) = \ell/2$ centered at its rotation center p, and the right-hand neighborhood contains one of radius $1+1/\sqrt{3} > \ell/2$. Therefore, RISC neighborhoods with rotation centers at a distance less than ℓ must overlap.

Two RISCs that overlap must do so in a union of tiles of $\mathcal{T}$, and their combinatorics constrain the possibilities. In particular, the left- and right-hand RISCs of Figure 8 can only overlap each other in a union of adjacent triangles, and this puts their centers at distance $1/\sqrt{3}+1+\sqrt{3}/2+1/(2\sqrt{3}) > \ell$. Therefore any two RISC neighborhoods with rotation centers at a distance less than ℓ must consist of two copies of the same type.

For overlapping copies of a single RISC type, their region of overlap either contains a square, or it is a union of two adjacent triangles. For the RISC on the left in Figure 8, the former region of overlap puts the rotation centers a distance of $1+1/\sqrt{3}$ apart, and the union of the two neighborhoods is pictured on the left in Figure 9. The latter puts the centers $1+2/\sqrt{3}$ apart and is pictured in the middle of the figure. For the RISC on the right in Figure 8, a region of overlap containing squares yields a distance of $1+2/\sqrt{3}$. This configuration is pictured on the right in Figure 9. On the other hand, overlapping in two adjacent triangles puts the distance at $1+\sqrt{3}+1/\sqrt{3} > \ell$, thus not satisfying the lemma's hypotheses. □

Proposition 5.8 *Suppose Λ is a discrete, cocompact group of orientation-preserving isometries of $\mathbb{R}^2$ containing rotations of order three that leaves invariant a tiling $\mathcal{T}$ of $\mathbb{C}$ into squares and equilateral triangles of sidelength 1 — with each shape represented — and such that the minimal translation length τ among infinite-order elements of Λ satisfies $\tau \leq 2+\sqrt{3}$. Then $\mathcal{T}$ is one of the tilings generated from those in Figure 9 as in Remark 5.7.*

Remark 5.9 The left-most tiling in Figure 9 is also pictured on the left in Figure 4; the center tiling as $\mathcal{S}$ in Figure 12; and the right-most as $\mathcal{R}$ in Figure 5.

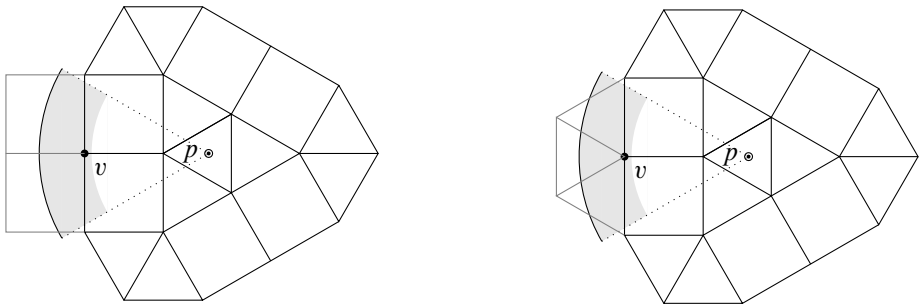

Figure 10: Two possible neighborhoods of a vertex v on $\partial(\mathrm{RISC})$.

Proof By Lemma 5.2, the fixed points of order-3 rotations of Λ lie on a lattice of equilateral triangles with sides of length $\tau/\sqrt{3}$. See Figure 9, where the relevant triangles are dashed. Fix a tile Δ of this tiling by equilateral triangles. Since $\mathcal{T}$ contains a square, by Corollary 5.5 at least one vertex of the tiling by equilateral triangles has a neighborhood in $\mathcal{T}$ isometric to one of those pictured in Figure 8, a RISC; therefore, by Lemma 5.2(1), at least one vertex of Δ has such a neighborhood.

If two vertices of Δ have RISC neighborhoods then since $\tau/\sqrt{3}$ is less than ℓ as defined in Lemma 5.6, that result plus Remark 5.7 imply the conclusion of this one. For the rest of this proof, we therefore consider the case that exactly one vertex of Δ, call it p, is a RISC rotation center. If e is the edge of Δ opposite p, $\bar{\Delta} \neq \Delta$ is the equilateral triangle sharing e with Δ, and $\bar{p}$ is the vertex of $\bar{\Delta}$ opposite e, then $\bar{p}$ is at distance τ from p and is its image under a translation belonging to Λ. It is thus also a RISC rotation center, and we may assume that $\tau \geq \ell$, for ℓ as in Lemma 5.6, since otherwise that result plus Remark 5.7 again classifies all possibilities.

We will show that in fact it is not possible for a unique vertex of Δ to be a RISC rotation center. We claim first:

Claim For $\ell \leq \tau \leq 2+\sqrt{3}$, if a unique vertex of Δ is a RISC rotation center, it does not belong to the RISC pictured on the right in Figure 8.

Proof of claim Consider possible locations of order-three rotation centers of Λ, relative to a ray ρ from the center p of the RISC pictured on the right in Figure 8 that splits a pair of its adjacent squares. Let v be the vertex of intersection between ρ and the RISC's boundary. The only two possible neighborhoods of v in $\mathcal{T}$ are pictured in Figure 10 — with either two squares (on the left) or three triangles (right) drawn in gray outside the RISC — along with an arc α of angular measure 60 degrees centered at the intersection between ρ and a circle of radius $1+2/\sqrt{3}$ centered at p. The shaded regions in the figure consist of points with these angular values and between circles of radii the upper and lower bounds on $\tau/\sqrt{3}$:

$$\frac{1}{3}+\frac{2}{\sqrt{3}} \leq \frac{\tau}{\sqrt{3}} \leq 1+\frac{2}{\sqrt{3}}.$$

At least one order-three rotation center of Λ must lie in the shaded region, since there are six such centers total, evenly spaced around the circle of radius $\tau/\sqrt{3}$ centered at p.

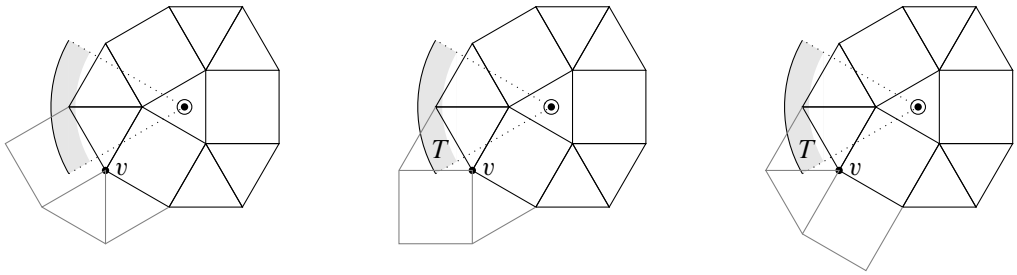

Figure 11: Possible rotation center locations.

The neighborhood of v pictured on the left in Figure 10 is not compatible with the existence of an order-three rotation center in the shaded region, since by Lemma 5.3, such a rotation center must occur at the centroid or a vertex of a triangle of $\mathcal{T}$. The neighborhood pictured on the right does encompass the case pictured on the right in Figure 9, in which the rotation center lies on the ray ρ at the centroid of the middle triangle, at a distance attaining the upper bound $1+2/\sqrt{3}$ for $\tau/\sqrt{3}$. In this case, applying the order-three rotation around this point and its inverse duplicates the previous figure. In particular, in this case there are distinct copies of this RISC centered at adjacent vertices; hence at adjacent vertices of Δ.

In the right-hand case of Figure 10, neither of the other two triangles outside the RISC can be preserved by an order-three rotation, since each intersects both a triangle and a square. And the parts of the shaded region that lie outside its intersection with the pictured neighborhood of v are contained in a union of squares and/or triangles that intersect both a square and a triangle. Thus no other location in the shaded region can be the fixed point of an order-three rotation that preserves $\mathcal{T}$, proving the claim. □

Given the claim, we are left to consider the RISC pictured on the left in Figure 8, in the case that $\ell \le \tau \le 2+\sqrt{3}$ and its center p is at the unique vertex of Δ which is a RISC rotation center. Hence as observed above, the nearest other RISC rotation center is a translate of this one at a distance τ away. A Euclidean geometry computation shows that this RISC type is entirely contained in a closed disk of radius $1+1/\sqrt{3}$ centered at p. If this is less than half of τ, then since every square tile of $\mathcal{T}$ is contained in a RISC (by Corollary 5.5), this RISC would intersect only triangles of $\mathcal{T}$. But this is not possible, since its boundary vertices which are contained in one square must also be contained in another. Therefore in this case we must have $2+2/\sqrt{3} \ge \tau \ge \ell \doteq 2+1/\sqrt{3}$.

In parallel to the proof of the above claim, we now consider possible locations of rotation centers at a distance of $\tau/\sqrt{3}$ from p. At least one must lie on a sixty-degree arc centered on a ray ρ from p that splits a pair of triangles that share an edge. Given the constraints on τ, this means that such a rotation center would lie in the shaded region(s) in Figure 11. This figure's three cases depict the three distinct possibilities for the combinatorics of a tiled neighborhood of the vertex labeled v on the RISC's boundary.

Since the RISC is invariant under reflection through the line containing ρ, after applying such a reflection if necessary, we may assume that there is a rotation center on the side of ρ containing v. We note first that such a rotation center cannot lie outside the pictured tiled neighborhood of v in any of the three cases, since in all cases the centroids of any other possible (not pictured) triangular tiles are not

close enough to p to lie in the shaded neighborhood. But the tiled neighborhood of v also cannot contain a rotation center in any of the three cases: in the leftmost, its intersection with the shaded neighborhood is contained in a square; in the other two its intersection with the shaded neighborhood contains the centroid of a unique triangle ("T" in Figure 11), but the neighborhood's combinatorics prohibit this centroid from being a rotation center for $\mathcal{T}$. In the center case we can see this from the fact that T shares one edge with a triangle and another with the square. In the right-hand case, while T shares edges only with triangles, one of these triangles abuts a square along its edge clockwise from its intersection with T, but the other one abuts a triangle along its corresponding edge.

Between this case and our claim, we have now shown that Δ cannot have a unique vertex that is a RISC rotation center. Therefore as discussed at the beginning of the proof, the classification of possibilities follows from Lemma 5.6 and Remark 5.7. □

6 Eliminating the remaining peripheral tiling

The main result of this section, Proposition 6.1 below, implies that the tiling $\mathcal{S}$ pictured in Figure 12 is not the peripheral tiling of a mixed-platonic knot complement with hidden symmetries. This holds even though the full orientation-preserving symmetry group of $\mathcal{S}$ is a $(2,3,6)$-rotation group, as will be explicitly exhibited in the proof of Proposition 6.1. It further implies the main Theorem 6.12, since $\mathcal{S}$ is the final possible peripheral tiling of such knots that has remained unaddressed to this point (the tilings $\mathcal{Q}$ and $\mathcal{R}$ were addressed in Corollary 4.5 and Proposition 4.7, respectively).

Proposition 6.1 *There is no orientable one-cusped, mixed-platonic orbifold $O = \mathbb{H}^3/\Gamma$ with peripheral tiling $\mathcal{S}$, such that the peripheral subgroup of Γ is the full orientation-preserving symmetry group $\mathrm{Sym}^{\mathrm{OP}}(\mathcal{S})$ of $\mathcal{S}$ or its index-two $(3,3,3)$-rotation subgroup.*

We will prove Proposition 6.1, and use it to complete the proof of the main theorem, in Section 6.2 below. Section 6.1 lays the foundation for this proof. It begins by reproducing the general definition of the Voronoi cell of a horoball in a horoball packing and culminates in Proposition 6.7, which characterizes the possible boundary faces of a Voronoi cell of a horoball packing supplied by Lemma 3.7 for an arbitrary mixed-platonic orbifold.

6.1 Voronoi tessellations of horoball packings

We begin by reproducing the definition of a standard tool in arguments about cusped hyperbolic 3-orbifolds since at least the work of Meyerhoff [26] identifying those of minimal volume. Given a horoball B_p centered at an ideal point p of $\mathbb{H}^3$, belonging to a horoball packing $\mathcal{H}$, the *Voronoi cell of B_p*, or when necessary, the *Voronoi cell of B_p relative to $\mathcal{H}$*, is defined as

$$V_p = \{x \in \mathbb{H}^3 \mid d(x, B_p) \leq d(x, B') \text{ for all } B' \in \mathcal{H}\}. \tag{2}$$

Its *interior* is $\mathrm{int}(V_p) = \{x \mid d(x, B_p) < d(x, B')\ \forall B' \neq B_p\}$, and its *boundary* is $V_p - \mathrm{int}(V_p)$. Some first observations about Voronoi cells, again very standard, are below.

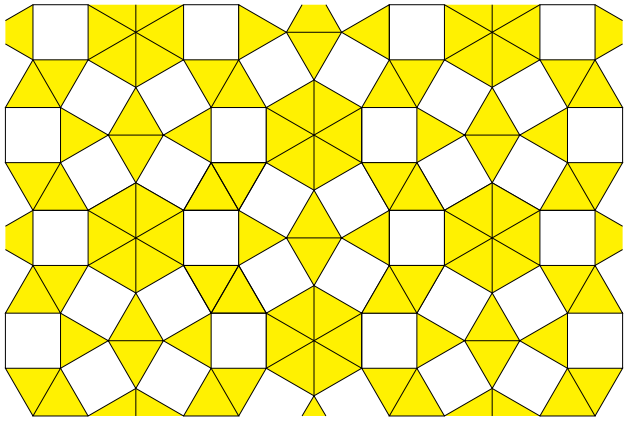

Figure 12: $\mathcal{S}$: the tiling of the plane where each square is surrounded by four triangles.

Fact 6.2 *Suppose $\mathcal{H}$ is a horoball packing of $\mathbb{H}^3$ and let $\partial_\infty\mathcal{H} = \{p \in \partial\mathbb{H}^3 \mid B_p \in \mathcal{H}\}$.*

- *For any $p \in \partial_\infty\mathcal{H}$, $B_p \subset V_p$ and $\mathbb{H}^3 = \bigcup_{p\in\partial_\infty\mathcal{H}} V_p$.*
- *If $\mathcal{H}$ is invariant under the action of a group Γ of isometries then so is the collection of Voronoi cells $\{V_p \mid p \in \partial_\infty\mathcal{H}\}$.*
- *For Γ as above, the stabilizer Λ of p in Γ equals the stabilizer of V_p.*
- *For Γ, p, and Λ as above, the restriction to V_p of the quotient map $\mathbb{H}^3 \to \mathbb{H}^3/\Gamma$ factors through a map of V_p/Λ that is an embedding on $\operatorname{int}(V_p)/\Lambda$.*

We next consider the very special case of a symmetric horoball packing centered at the ideal points of a regular ideal tetrahedron or octahedron. We first make a definition.

Definition 6.3 Given a pair of nonoverlapping horoballs B_p and B_q, let λ be the geodesic joining p to q; let x be the point of λ equidistant from B_p and B_q; and define H_{pq} to be the half-space that is bounded by the geodesic plane that intersects λ perpendicularly at x and contains B_p.

A standard exercise in hyperbolic trigonometry shows that the half-space H_{pq} of Definition 6.3 consists exactly of the points of $\mathbb{H}^3$ that are at least as close to B_p as to B_q. In particular, H_{pq} contains B_p. It further follows from this property and the definition that if B_p belongs to a horoball packing $\mathcal{H}$ then

$$V_p = \bigcap_{q\in\partial_\infty\mathcal{H}-\{p\}} H_{pq}. \tag{3}$$

We use this characterization below.

Lemma 6.4 *For P a regular ideal tetrahedron or octahedron, let $\mathcal{H}_P$ be the maximal, fully symmetric horoball packing centered at the ideal vertices of P from Definition 3.4. If $P = T$ is a regular ideal tetrahedron then for a fixed ideal vertex p of T, enumerating the other ideal vertices of T as q_1, q_2 and q_3, the Voronoi cell $V_p = H_{pq_1} \cap H_{pq_2} \cap H_{pq_3}$ of B_p relative to $\mathcal{H}_T$ does not intersect the face of T containing q_1, q_2 and q_3.*

If $P = O$ is a regular ideal octahedron then for a fixed ideal vertex p of O, the Voronoi cell V_p of B_p is $H_{pq_1} \cap H_{pq_2} \cap H_{pq_3} \cap H_{pq_4}$, where q_1, q_2, q_3 and q_4 are the other distinct ideal vertices of O that are joined to p by an edge of O. V_p intersects only the faces of O that contain p.

In each case, V_p has an angle of $2\pi/3$ at each of its edges, which are of the form $\partial H_{pq_i} \cap \partial H_{pq_j}$ for $j \neq i$ such that q_i and q_j are ideal vertices of a common face of $P = T$ or O. It has a single vertex $v = \bigcap_i \partial H_{pq_i}$. The nearest-point retraction to B_p takes v to the centroid of the equilateral triangle or square $P \cap \partial B_p$, and the edges of V_p into equidistant lines between adjacent vertices of $P \cap \partial B_p$.

Proof In the case of the regular ideal tetrahedron T, working in the upper half-space model for $\mathbb{H}^3$ we may assume that the ideal vertices are $p = \infty$, $q_1 = 0$, $q_2 = 1$, and $q_3 = \omega$, where $\omega = \frac{1}{2}(1 + i\sqrt{3})$. The horoball packing $\mathcal{H}_T$ then has B_∞ as the region above the Euclidean plane of height one, with each B_{q_i} a ball of Euclidean radius $1/2$ tangent to $\mathbb{C} \times \{0\}$ at q_i. For each i, H_{pq_i} is then the region above a Euclidean hemisphere of radius 1 centered at q_i.

Points of the Euclidean hemisphere ∂H_{pq_i} are of the form (z, t), where $t = \sqrt{1 - \|z - q_i\|^2}$ for $\|z - q_i\|$ the Euclidean distance from z to q_i in $\mathbb{C}$. Such a point (z, t) thus lies in V_p if and only if z is at least as close to q_i as to any other q_j, since if this were not the case it would lie outside of H_{pq_j}. The edges of V_p are of the form $\partial H_{pq_i} \cap \partial H_{pq_j}$, for $j \neq i$, and it follows that these consist of points (z, t) such that z is Euclidean-equidistant from both q_i and q_j. This also describes their images under projection to B_∞ which in the present model is the map $(z, t) \mapsto (z, 1)$. A Euclidean geometry computation further shows that the angle between ∂H_{pq_i} and ∂H_{pq_j} along their geodesic of intersection is $2\pi/3$.

Finally, the lowest point of $V_p \cap T$ occurs at the point (z, t) such that z has maximum distance from the q_i, the triple intersection point

$$v = \bigcap_{i=1}^{3} \partial H_{pq_i} = \left\{ \left(\frac{1}{2} + \frac{\sqrt{3}}{6} i, \sqrt{\frac{2}{3}} \right) \right\}.$$

This lies above the geodesic plane containing the face of T opposite $p = \infty$, which is a Euclidean hemisphere of radius $1/\sqrt{3}$. We finally note that the projection of v to ∂B_∞ is equidistant from the three vertices 0, 1, and ω of $T \cap \partial B_\infty$.

We can likewise embed the regular ideal octahedron O in the upper half-space model for $\mathbb{H}^3$ with its vertex p at ∞ and q_1 through q_4 at 0, 1, $1 + i$, and i in (say) counterclockwise order. This embedding places the final vertex p' of O, the one opposite p, at $(1 + i)/2$. As for $\mathcal{H}_T$, with this embedding $B_\infty \in \mathcal{H}_O$ is the region above the plane at height 1, the B_{q_i} are Euclidean balls of radius $1/2$, and the H_{pq_i} lie above Euclidean hemispheres of radius 1.

Note that in this case, for i and j such that q_i and q_j are opposite vertices of the square bounded by all of the q_i then every point of $\partial H_{pq_i} \cap \partial H_{pq_j}$ lies beneath ∂H_{pq_k} for some $k \neq i, j$, save the unique quadruple intersection point

$$v = \bigcap_{i=1}^{4} \partial H_{pq_i} = \left\{ \left(\frac{1 + i}{2}, \frac{1}{\sqrt{2}} \right) \right\}.$$

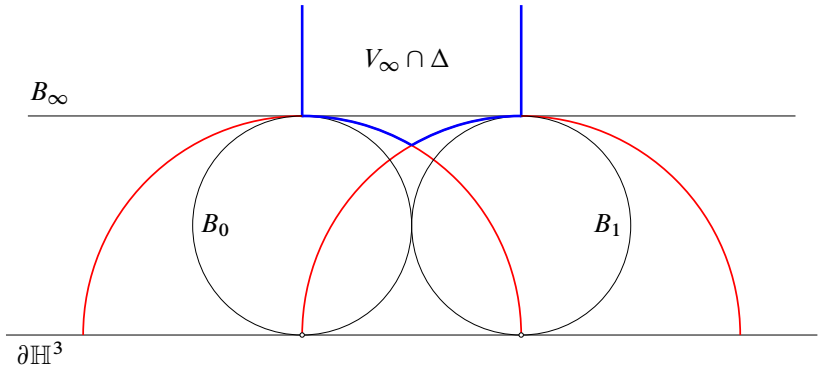

Figure 13: $V_\infty \cap \Delta$ outlined in blue, where Δ is the face with vertices at 0, 1 and ∞ of a regular ideal tetrahedron or octahedron in standard position as in Definition 3.1. Also showing horoballs centered at 0, 1 and ∞ belonging to the associated packing $\mathcal{H}_T$ or $\mathcal{H}_O$ from Lemma 6.4, or $\mathcal{H}$ from Lemma 3.7, and cross-sections of equidistant planes in red.

Therefore $\partial H_{pq_i} \cap \partial H_{pq_j}$ contains an edge of $\bigcap_{i=1}^4 H_{pq_i}$ if and only if q_i and q_j are adjacent vertices of the square, i.e., if and only if they are ideal vertices of a face of O.

The quadruple intersection point v above is also the lowest point of $\bigcap_{i=1}^4 H_{pq_i}$, as its z coordinate maximizes the distance to all q_i. The Euclidean hemisphere of radius $1/\sqrt{2}$ centered at $(1+i)/2$, which contains v, also contains all q_i in its ideal boundary. Furthermore the reflection in this hemisphere exchanges $p = \infty$ with $p' = (1+i)/2$, fixing the q_i. This reflection therefore acts as a symmetry of O which, by the symmetry-invariance of $\mathcal{H}_O$, exchanges B_p with $B_{p'}$. It follows that $H_{pp'}$ is the region above the fixed set of this reflection, so by the above, $H_{pp'}$ contains $\bigcap_{i=1}^4 H_{pq_i}$. Therefore,

$$V_p = H_{pp'} \cap \left(\bigcap_{i=1}^4 H_{pq_i} \right) = \bigcap_{i=1}^4 H_{pq_i}.$$

For the assertion that V_p intersects only the faces of O containing p, we note that $\partial H_{pp'}$ separates V_p from the remaining three faces, which all contain p'. The assertions about the dihedral angles at edges, and their projections and that of v, follow as in the previous case. □

For reference, Figure 13 shows the view of $V_p \cap \Delta$ "from the side", and Figure 14 records the "view from infinity" of $(\partial V_p) \cap T$ and $(\partial V_p) \cap O$ in the two cases of Lemma 6.4, with the polyhedra embedded as in that lemma's proof with p at ∞. Taking "P" to represent T or O in the respective cases, the portion of $(\partial V_p) \cap P$ contained in H_{pq_1}, with q_1 at 0, is shaded in each case, and the bold arcs represent segments of pairwise intersections $\partial H_{pq_i} \cap \partial H_{pq_j}$ that are contained in $(\partial V_p) \cap P$.

Figure 14: The intersection of a Voronoi cell's boundary with a single polyhedron.

Lemma 6.5 *Suppose $O = \mathbb{H}^3/\Gamma$ is a mixed-platonic 3-orbifold, and let $\mathcal{P}$ be a Γ-invariant tiling of $\mathbb{H}^3$ by regular ideal tetrahedra or octahedra. For any tile P of $\mathcal{P}$, and any $x \in P$, each closest horoball to x among all those in the horoball packing $\mathcal{H}$ supplied by Lemma 3.7 is centered at an ideal vertex of P. Thus for any ideal vertex p of P, with horoball $B_p \in \mathcal{H}$ centered at p, $V_p \cap P = V_p^P \cap P$, where V_p and V_p^P are the Voronoi cells of B_p respectively relative to $\mathcal{H}$ and to the packing $\mathcal{H}_P$ from Definition 3.4.*

Proof First fix a tile P of $\mathcal{P}$ and $x \in P$, and by way of contradiction suppose there is a nearest horoball B of $\mathcal{H}$ to x with its center not at an ideal vertex of P. Let λ be the arc from x to its nearest point on B, and let P_0 be the tile containing $\lambda \cap B$. Lemma 3.7 implies that B does not intersect P, so $P_0 \neq P$, and that the center of B is an ideal vertex p_0 of P_0. The sides of P_0 intersecting B contain this ideal vertex and intersect ∂B at right angles. Because B is convex and $\lambda \cap B$ is the closest point on B to x, λ also intersects ∂B at right angles. Therefore the point x_0 where it exits P_0 is contained in a face f_0 of P_0 that does not have the center of B as an ideal vertex. By Lemma 6.4, x_0 is closer to a horoball B_1 centered at an ideal point of f_0 than to B. The distance $d(x, B_1)$ from x to B_1 is at most the sum of $d(x, x_0)$ and $d(x_0, B_1)$, and this is less than $d(x, B) = d(x, x_0) + d(x_0, B)$. But this contradicts the hypothesis that B is the closest horoball of $\mathcal{H}$ to x.

For the final assertion we first recall from the proof of Lemma 3.7 that $\mathcal{H} = \bigcup_{P \in \mathcal{P}} \mathcal{H}_P$. The characterization (3) therefore immediately implies that $V_p \subseteq V_p^P$, since V_p is an intersection of half-spaces determined by a proper subset of the horoballs in $\mathcal{H}$. To give the other containment for their intersections with $\mathcal{P}$ we appeal to the lemma's first assertion: for any $x \in P$, since the nearest horoball to x lies in the collection $\mathcal{H}_P$, $x \in V_p$ if and only if $x \in V_p^P$. □

Corollary 6.6 *Let $M = \mathbb{H}^3/\Gamma$ with a Γ-invariant tiling $\mathcal{P}$ of $\mathbb{H}^3$ by tetrahedra and octahedra. Then $\mathcal{P}$ is the **canonical cell decomposition** of the horoball packing $\mathcal{H}$ supplied by Lemma 3.7 in the sense described above* [15, Theorem 2.4] *(building on the one-cusped case laid out by Epstein and Penner* [13, Section 4]*).*

Proof As described in [15], the canonical cell decomposition of $\mathcal{H}$ is dual to its "Ford spine", which, per the definition given there, is identical to the union of boundaries of the Voronoi cells defined here in (2). Specifically, the canonical 3-cell dual to a vertex v of the Ford spine is the convex hull of the set of centers of horoballs whose Voronoi cells have v as a vertex.

The final assertion of Lemma 6.5 implies that the set of vertices of Voronoi cells relative to $\mathcal{H}$ is the union, over all $P \in \mathcal{P}$ and ideal vertices p of P, of the vertices of the Voronoi cell V_p of B_p relative to $\mathcal{H}_p$. Lemma 6.4 implies that there is a unique such vertex v_P for each $P \in \mathcal{P}$, which lies in the intersection of all V_p for ideal vertices p of P. By the first assertion of Lemma 6.5, v_P does not lie in any other Voronoi cell. Therefore P — which is the convex hull of its ideal vertices — is the dual to v_P. □

Our next result implies that if $\mathcal{T}$ is a peripheral tiling of a mixed-platonic orbifold O then the structure of the Voronoi cell of the corresponding cusp of O is entirely determined by $\mathcal{T}$. The terminology of convex polyhedra and sides are used as in [29, Section 6.2].

Proposition 6.7 *Suppose $\mathcal{T}$ is a peripheral tiling of a mixed-platonic orbifold $O = \mathbb{H}^3/\Gamma$. With Γ represented in standard position as prescribed in Definition 4.1, let $\mathcal{P}$ be a Γ-invariant tiling of $\mathbb{H}^3$ such*

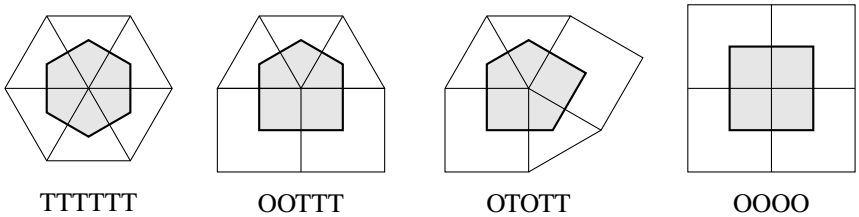

Figure 15: The four types of possible projected Voronoi faces of a peripheral tiling.

that $\mathcal{T} = \mathcal{P} \cap \partial B_\infty$, where B_∞ is the horoball at ∞ of the packing $\mathcal{H}$ supplied by Lemma 3.7. Then the Voronoi cell V_∞ of B_∞ is a convex polyhedron. Its collection of sides corresponds bijectively with the set of edges of $\mathcal{P}$ that have one ideal vertex at ∞, and has the following further properties:

(1) *for any two faces meeting along an edge, the dihedral angle in V_∞ is $2\pi/3$ along this edge*; *and*

(2) *the collection of faces projects to ∂B_∞ along geodesics orthogonal to it, and its image is a tiling of $\mathbb{R}^2$ dual to $\mathcal{T}$: the Voronoi tessellation of the set of vertices of $\mathcal{T}$, defined as in (2) but with vertices replacing horoballs.*

Each two-cell of the tiling of ∂V_∞ is drawn from among the tile types pictured in Figure 15, labeled according to the sequence of types of tiles of $\mathcal{P}$ encountered in cyclic order around the corresponding edge of $\mathcal{P}$.

Proof For $\mathcal{P}$ and $\mathcal{H}$ as in the proposition statement, and any $P \in \mathcal{P}$, let $\mathcal{H}_P$ be the finite set consisting only of those horoballs of $\mathcal{H}$ which are centered at ideal vertices of P. By Lemma 6.5, if $P \in \mathcal{P}$ has ∞ as an ideal vertex then $V_\infty \cap P = V_\infty^P \cap P$, where V_∞^P is the Voronoi cell of B_∞ relative to the horoball packing $\mathcal{H}_P$ of Definition 3.4. This implies that V_∞ is a polyhedron: for any compact set K intersecting V_∞, $K \cap V_\infty$ is contained in the union $P_1 \cup \ldots \cup P_n$ of finitely many members of $\mathcal{P}$, and for any such $P_j = P$, by the claim there are either three or four geodesic planes ∂H_{pq_i} (notation from the proof of Lemma 6.4, with $p = \infty$) whose union contains $\partial V_\infty \cap P$. It therefore follows that $K \cap \partial V_\infty$ intersects only the finite collection of sides that have the form $\partial H_{pq_i} \cap V_\infty$, taken over all such $P = P_j$ and their associated H_{pq_i}.

For the characterization of the sides, i.e., two-dimensional faces, we begin by recalling that by the definition of $\mathcal{H}$ in Lemma 3.7, for each polyhedron P as above and each edge e of P with an ideal endpoint at ∞, there is another horoball B_q of $\mathcal{H}_P$ centered at the other ideal endpoint q of e and a point of tangency $B_\infty \cap B_q = \{x\} \subset e$. Because x is a point of tangency, there is an open neighborhood of x in the totally geodesic plane $\partial H_{\infty q}$ (as in Definition 6.3) consisting of points for which B_q and B_∞ are the only closest members of $\mathcal{H}$; which therefore lie in $F_e := H_{\infty q} \cap \partial V_\infty$. The intersection of F_e with each polyhedron $P' \in \mathcal{P}$ containing e has the form of one of the kites pictured in Figure 14, and the union of these kites forms one of the polygons of Figure 15. (These reflect all combinatorial possibilities for the arrangement of regular ideal tetrahedra and octahedra containing a single edge.)

The assertion about the dihedral angle of V_∞ along any of its edges, and the characterization of ∂V_∞ as the Voronoi tessellation of the vertices of $\mathcal{T}$, both now follow directly from Lemma 6.4. □

The observation below concerns the pentagons of Figure 15.

Lemma 6.8 *Let B be a horoball of a packing $\mathcal{H}$ associated to an orientable mixed-platonic orbifold $\mathbb{H}^3/\Gamma$ as in Lemma 3.7, centered at ideal vertices of a Γ-invariant tiling $\mathcal{P}$, and let V be the Voronoi cell of B relative to $\mathcal{H}$. For any pentagonal faces F and F' of the tiling of ∂V described in Proposition 6.7, such that $\gamma(F) = F'$ for some $\gamma \in \Gamma$, F and F' have the same type, and γ takes the unique edge of F that joins the centers of two octahedra (if F is of type OOTTT) or tetrahedra (if type OTOTT) to the corresponding edge of F'. In particular, the only nontrivial self-isometry of either pentagon type is a reflection fixing the edge specified above.*

Proof This follows essentially by inspection of Figure 15, upon recalling that the lighter-outlined squares and triangles there represent the horospherical cross-sections of tiles of $\mathcal{P}$ by ∂B. Every element of Γ takes tiles of $\mathcal{P}$ to tiles of $\mathcal{P}$, and if γ takes F to F' then it takes the edge of $\mathcal{P}$ corresponding to F, with one ideal point at the center of B, to the edge of $\mathcal{P}$ corresponding to F'. □

6.2 The proof of Proposition 6.1

We begin with a lemma that builds on the previous subsection's results.

Lemma 6.9 *Let B be a horoball of a packing $\mathcal{H}$ associated to an orientable mixed-platonic orbifold $\mathbb{H}^3/\Gamma$ as in Lemma 3.7, centered at ideal vertices of a Γ-invariant tiling $\mathcal{P}$, and let V be the Voronoi cell of B relative to $\mathcal{H}$. For a face F of V and an edge e of F such that an element $\gamma \in \Gamma$ outside the stabilizer Λ of B stabilizes e and F, let F_0 be the face of V that shares the edge e, and let $B_0 \neq B$ be the horoball that is tangent to B in the interior of F_0. Then γ stabilizes B_0 and its ideal point.*

Proof For B, V, F, e, and γ as in the hypothesis, since γ lies outside Λ it is nontrivial. Because it stabilizes F and e it must act nontrivially on e: if it fixed e then since it preserves the normal direction pointing into F it would also fix F; hence since it preserves orientation it would fix all of $\mathbb{H}^3$. Thus it acts on e as reflection through its midpoint. Since it stabilizes F but not B it must exchange B with the horoball B' of $\mathcal{H}$ tangent to B in the interior of F; hence acting as a 180-degree rotation around the perpendicular bisector of e in the hyperplane containing F.

By Proposition 6.7, each Voronoi cell containing e has a dihedral angle of $2\pi/3$ along e; therefore there are exactly three such Voronoi cells. Since each of V, the Voronoi cell V' of B', and the Voronoi cell V_0 of the horoball B_0 identified in the lemma's statement contains e, these must be the only three. Since γ takes e to itself it preserves the collection of horoballs whose Voronoi cells contain e. It exchanges B with B', by the paragraph above, so it must stabilize B_0 and therefore also its ideal point. □

The result below takes for granted the fact that a discrete group Γ such that $\mathbb{H}^3/\Gamma$ has *one cusp* acts transitively on an associated Γ-invariant horoball packing.

Corollary 6.10 *Suppose $O = \mathbb{H}^3/\Gamma$ is an orientable one-cusped mixed-platonic orbifold and B is a horoball of the packing $\mathcal{H}$ associated to O by Lemma 3.7, with Voronoi cell V and stabilizer $\Lambda \subset \Gamma$. If there exist a face F of V and edge e of F both stabilized by some $\gamma \in \Gamma - \Lambda$, then Λ contains two-torsion.*

Proof With the given hypothesis, Lemma 6.9 identifies a horoball B_0 of $\mathcal{H}$ such that γ stabilizes B_0 and its ideal point. Because O has one cusp, Γ acts transitively on $\mathcal{H}$, so there exists $\delta \in \Gamma$ taking B_0 to B. Then $\delta\gamma\delta^{-1}$ is an order-two element of Λ. □

Recall the statement of Proposition 6.1:

Proposition 6.1 *There is no orientable one-cusped, mixed-platonic orbifold $O = \mathbb{H}^3/\Gamma$ with peripheral tiling $\mathcal{S}$, such that the peripheral subgroup of Γ is the full orientation-preserving symmetry group $\mathrm{Sym}^{\mathrm{OP}}(\mathcal{S})$ of $\mathcal{S}$ or its index-two $(3,3,3)$-rotation subgroup.*

Proof Suppose that there is an orientable, one-cusped orbifold $O = \mathbb{H}^3/\Gamma$ such that $\mathcal{S}$ is the peripheral tiling of O in the sense of Definition 4.1. That is, with Γ in standard position as in Definition 3.1, $\mathcal{S} = \mathcal{P} \cap \partial B_\infty$, where $\mathcal{P}$ is a Γ-invariant tiling by regular ideal tetrahedra and octahedra and B_∞ is the horoball centered at ∞ of the Γ-invariant horoball packing $\mathcal{H}$ supplied by Lemma 3.7. Let V_∞ be the Voronoi cell of B_∞. If $\Lambda < \Gamma$ is the stabilizer of ∞ then restricting its action to ∂B_∞ exhibits Λ as a subgroup of $\mathrm{Sym}^{\mathrm{OP}}(\mathcal{S})$.

The Voronoi cells of the horoballs of $\mathcal{H}$ tile $\mathbb{H}^3$ and, since O has a single cusp, Γ acts transitively on these cells. This implies that the restriction of the universal cover to V_∞ factors through a map of V_∞/Λ ultimately mapping onto O. The interior of V_∞ embeds in O under this map. These assertions follow from Fact 6.2. The boundary of V_∞ is tiled by totally geodesic hexagons and pentagons whose edges have finite length. Λ acts on ∂V_∞ preserving the tiling, taking edges to edges and faces to faces. If $\gamma \in \Lambda$ and e is an edge of this tiling, there are only two possibilities for the map $\gamma : \gamma^{-1}(e) \to e$ and they differ by the order-2 reflection of e through its midpoint. This means that each edge can be broken into two edges by adding midpoints as vertices and Λ acts on this graph of half-edges taking edges to edges and vertices to vertices. The dihedral angle of ∂V_∞ at any given half-edge is $2\pi/3$ and it follows that the total angle in O around the image of a given half-edge e of ∂V_∞ is $m \cdot 2\pi/3$, where m is the number of distinct Λ-orbits of half-edges identified to e in O. Because O is a hyperbolic orbifold, the total angle around any half-edge quotient in O must be an integer submultiple of $2\pi/n$ of 2π, where n is the order of the edge stabilizer in Γ. This means that, for any half-edge e of ∂V_∞, the number of distinct Λ-orbits of half-edges identified to e in O is either one or three.

Notice that every (full) edge of ∂V, for any given Voronoi cell associated to $\mathcal{H}$, either has endpoints contained in a pair of adjacent tetrahedra or in an adjacent pair of an octahedron and a tetrahedron. Edges of the first type will be called *short* and of the second type *long*. Because Γ preserves the mixed platonic tiling of $\mathbb{H}^3$, the action of Γ on the set of edges of faces of Voronoi cells respects this edge classification. In particular, any orbit containing a short half-edge contains exclusively short half-edges.

Suppose that Λ is the full OP symmetry group of $\mathcal{S}$. Then Λ is a $(2,3,6)$-rotation group and the gray triangle D in Figure 16 is a fundamental domain for its action on ∂V_∞. In the figure, the tiles of $\mathcal{S}$ which

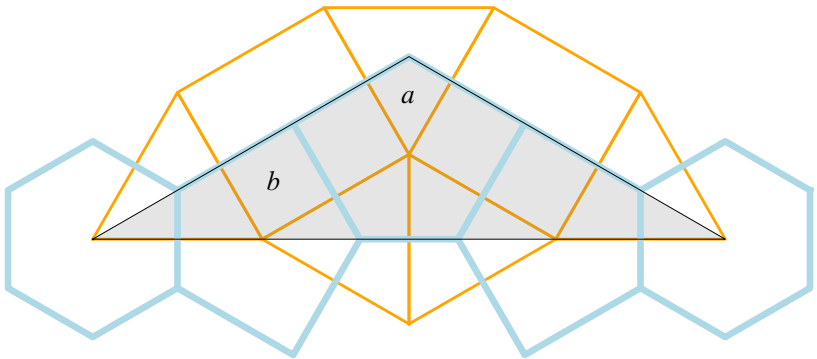

Figure 16: A fundamental domain for the $(2,3,6)$-rotation group $\mathrm{Sym}^{\mathrm{OP}}(\mathcal{S})$ of symmetries of $\mathcal{S}$.

intersect D are shown in orange and the faces of ∂V_∞ which intersect D are shown in light blue. Let σ be the order-2 elliptic isometry whose axis is vertical and pierces the horizontal edge of D.

Inspecting Figure 16, we find that the tiling of ∂V_∞ by pentagons and hexagons has two Λ-orbits of pentagons, represented by the pentagons labeled a and b. There is a single Λ-orbit of hexagons. Name the leftmost hexagon in Figure 16 as h and set $t = h \cap D$. Let V_h, V_a and V_b be the Voronoi cells that meet V_∞ along h, a and b. Let e be the upper half of the short edge of b. Our goal is to show, for a contradiction, that the number of distinct Λ-orbits of half-edges identified to e in O cannot be one or three.

Since Γ acts transitively on the tiling by Voronoi cells, there is an element $\gamma_1 \in \Gamma$ which takes V_∞ to V_b. Let X be the pentagon $\gamma_1^{-1}(b)$. Then $\gamma_1(X) = b$. Since X belongs to the Λ-orbit of either a or b, by precomposing γ_1 by an element of Λ, we may assume $X \in \{a, b\}$. Similarly, there is an element $\gamma_2 \in \Gamma$ which takes V_∞ to V_h. As before, we may assume that $\gamma_2^{-1}(t) \subset D$ and, since γ_2 acts as an OR isometry (using the induced boundary orientation from V_∞), it must be true that $\gamma_2^{-1}(t)$ is the triangle $\sigma(h) \cap D$.

The dihedral angles of V_∞, V_b, and V_h at e are all $2\pi/3$, so V_b and V_h intersect at a face F that contains e. Because $\gamma_2^{-1}(V_h) = V_\infty$ and $\gamma_2^{-1}(h) = \sigma(h)$, the pentagon $\sigma(b)$ is $\gamma_2^{-1}(F)$. Therefore, $V_\infty = \gamma_1^{-1}(V_b)$ has a pentagonal face across $\gamma_1^{-1}(e)$ from X and so X must be a.

Note that there are a total of 8 Λ-orbits of long half-edges. However, upon combining the effects of γ_1 on the edges of a and b with the action of Λ, we find that four of these orbits are identified under the action of Γ. Since there should only be three, this is a contradiction.

To finish, suppose that Λ is the index-2 $(3,3,3)$-rotation subgroup of $\mathrm{Sym}^{\mathrm{OP}}(\mathcal{S})$. The gray diamond D' in Figure 17 is a fundamental domain for the action of Λ on ∂V_∞. The tiling of ∂V_∞ by geodesic hexagons and pentagons has four Λ-orbits of pentagons which are represented by a, b, and their images under σ. We name the leftmost hexagon in Figure 17 as h, as in the $(2,3,6)$ case, and let t' be the triangle $h \cap D'$.

Naming the Voronoi cells adjacent to V_∞ as V_a, V_b, and V_h as before, and taking $\gamma_2 \in \Gamma$ to be an element with $\gamma_2(V_\infty) = V_h$ and $\gamma_2^{-1}(t') \in D'$, in this case (unlike the previous one) it is a priori possible that $\gamma_2(t') = t'$. However if this were so then γ_2 would stabilize h and the edge e of h contained in t', so Λ would contain two-torsion by Corollary 6.10, contradicting that it is a $(3,3,3)$-rotation group. Therefore $\gamma_2^{-1}(t') = \sigma(t')$, analogous to the first case.

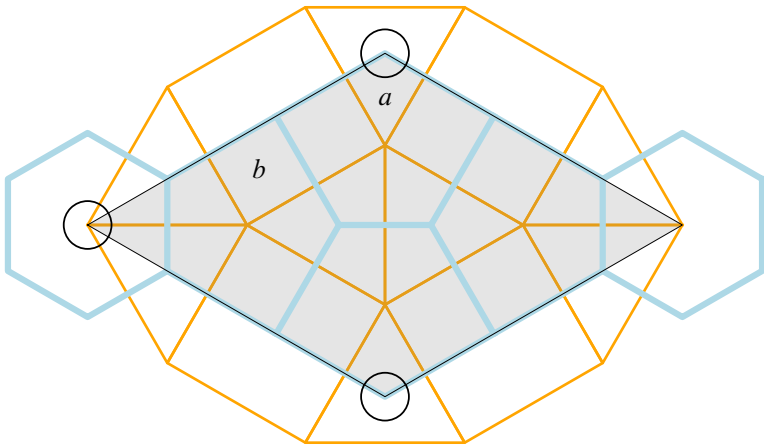

Figure 17: A fundamental domain for the $(3,3,3)$-rotation group that is the unique index-two subgroup of $\mathrm{Sym}^{\mathrm{OP}}(\mathcal{S})$.

Now following the argument from the first case, we find an element $\gamma_1 \in \Gamma$ which takes V_∞ to V_b so that $\gamma_1(X) = b$ for some $X \in \{a, \sigma(a)\}$. Applying the same argument to $\sigma(b)$, on the right half of the domain D', we find an element $\gamma_1' \in \Gamma$ which takes V_∞ to $V_{\sigma(b)}$ so that $\gamma_1'(Y) = \sigma(b)$ for some $Y \in \{b, \sigma(b)\}$. Now, if $X = Y$, then $\gamma_1'\gamma_1^{-1}(b) = \sigma(b)$ and $\gamma_1'\gamma_1^{-1}(V_b) = V_{\sigma(b)}$ and together these imply that $\gamma_1'\gamma_1^{-1}$ fixes ∞. But then $\gamma_1'\gamma_1^{-1} \in \Lambda$ and identifies the distinct Λ-orbits represented by b and $\sigma(b)$, a contradiction. Therefore, X and Y must be distinct in $\{a, \sigma(a)\}$.

From here, our proof assesses the number of Λ-orbits of long half-edges which are identified to single half-edges in O. The argument is undisturbed by the horizontal reflection of the diamond D', so we may assume $X = a$ and $Y = \sigma(a)$.

Now again, upon combining the effects of γ_1 and γ_1' on the Λ-orbits of long half-edges with the action of Λ, we find that more than three of these orbits are identified to a single edge in O under the action of Γ. Since there should only be three, this is a contradiction and our proof is complete. □

Corollary 6.11 *There is no mixed-platonic knot whose complement has hidden symmetries and peripheral tiling $\mathcal{S}$.*

Proof Suppose $M = \mathbb{H}^3/\Gamma_K$ is the complement of a mixed-platonic knot K, with peripheral tiling $\mathcal{S}$, and let B be a horoball of the associated packing from Definition 4.1. Recalling that each equilateral triangle and square edge of $\mathcal{S}$ has length 1 on ∂B, we compute that the shortest distance between distinct vertices of $\mathcal{S}$ that are shared by six triangles is $2+\sqrt{3}$. Since the peripheral subgroup Λ_K of M preserves $\mathcal{S}$, it takes any such vertex to another. By Lemma 3.17, an element μ of Λ_K representing a meridian of K has translation length exactly $2+\sqrt{3}$ and hence takes any such vertex v to another vertex at minimal distance from it.

If M has hidden symmetries then it covers a rigid cusped orbifold $O = \mathbb{H}^3/\Gamma$, for a discrete group Γ containing Γ_K, with a $(2,3,6)$- or $(3,3,3)$-rigid cusp [20]. Proposition 3.9 implies that O also has $\mathcal{S}$ as

its peripheral tiling. Let Λ be the peripheral subgroup of Γ containing Λ_K. If Λ is a $(2,3,6)$-rotation group then we claim it must be the full symmetry group $\mathrm{Sym}^{\mathrm{OP}}(\mathcal{S})$ of $\mathcal{S}$, contradicting Proposition 6.1.

To see this, let ρ_0 be an order-six element of Λ, and let $\rho_1 = \mu\rho_0\mu^{-1}$. The fixed points of the ρ_i are each valence-six vertices of $\mathcal{S}$, at distance $2+\sqrt{3}$ from each other. Hence inspecting $\mathcal{S}$ we find that $\sigma = \rho_0\rho_1$ is an order-three rotation fixing the center of one of the equilateral triangles of $\mathcal{S}$ adjacent to three squares that is closest to the midpoint of the segment joining the fixed point of ρ_0 to that of ρ_1. Then $\langle\rho_0,\sigma\rangle = \mathrm{Sym}^{\mathrm{OP}}(\mathcal{S})$, by coarea for example, proving the claim.

We now claim that if Λ is a $(3,3,3)$-rotation group then it is the index-two $(3,3,3)$-subgroup of $\mathrm{Sym}^{\mathrm{OP}}(\mathcal{S})$, again contradicting Proposition 6.1. To see this, let ρ be an order-three rotation of Λ with fixed point c. One can see directly that the composition $\rho\mu$ fixes a point c' at distance $(2+\sqrt{3})/\sqrt{3}$ from c. This is the smallest distance between any two distinct points fixed by order-three rotations in $\mathrm{Sym}^{\mathrm{OP}}(\mathcal{S})$. Therefore up to the $\mathrm{Sym}^{\mathrm{OP}}(\mathcal{S})$-action, c and c' are among the vertices of the fundamental domain in Figure 17 circled in black. Then ρ and $\rho\mu$ generate the index-two $(3,3,3)$-subgroup of $\mathrm{Sym}^{\mathrm{OP}}(\mathcal{S})$. □

The result above is the final ingredient in the proof of this paper's main theorem:

Theorem 6.12 *No mixed-platonic knot complement in S^3 has hidden symmetries.*

Proof Suppose $\mathcal{T}$ is the peripheral tiling of a mixed-platonic knot complement with hidden symmetries. By Proposition 5.1, $\mathcal{T}$ is a tiling of $\mathbb{R}^2$ by unit-sidelength squares and equilateral triangles possessing both order-3 rotational symmetry and a translational symmetry of length at most $2+\sqrt{3}$. Proposition 5.8 therefore implies that $\mathcal{T}$ is one of $\mathcal{Q}$, $\mathcal{R}$, or $\mathcal{S}$ (the three tilings generated from those in Figure 9 as in Remark 5.7). However none of these can be the peripheral tiling of M by Corollary 4.5, Proposition 4.7, and Corollary 6.11, respectively, moving from left to right across the figure. This contradiction finishes the proof. □

7 Questions

The full class of mixed-platonic manifolds remains generally mysterious beyond the known examples described in Section 2. For instance the following is open to our knowledge:

Question 7.1 *Are there mixed-platonic knots other than* $12n706$*? Are there infinitely many*?

By Lemma 3.2, every mixed-platonic knot complement has the quartic invariant trace field $\mathbb{Q}(i,\sqrt{-3})$. While the hybridization construction discussed in Example 2.5 produces infinite families of link complements with this invariant trace field, and one can also produce infinite families of *two component* link complements having the same quartic invariant trace fields (see [10]), it seems that there are no known infinite families of knot complements with the same trace field. Indeed, while small finite families of knot complements with the same quartic trace fields have been observed computationally (for example the complements of $6a3$, $7a1$, and $9a7$ in the `HTLinkExteriors` census), these computations could best be described as observations and do not seem to lead to any kind of constructive method.

In another algebraic direction, since mixed-platonic knot complements have representations in the cyclotomic ring of integers $\mathbb{Z}[\zeta_{12}]$ (see Proposition 3.13), we ask:

Question 7.2 *Are there knot complements other than those of the figure-eight and $12n706$ with representations in the ring of integers of a cyclotomic field*?

One way to shed light on the questions above would be to answer the one below, which can likely be attacked using current computational methods.

Question 7.3 *What is the classification of one-cusped mixed-platonic manifolds of low volume or complexity*? *What is their* ***commensurability*** *classification*?

Regarding the commensurability classification, we note that any two platonic manifolds that decompose into copies of the same platonic solid — e.g., any two tetrahedral manifolds — are commensurable, but this is very much not the case for mixed-platonic manifolds. For instance, the Boyd knot complement of Example 2.7 is not commensurable with $s913$ from Example 2.8: the former has a mixed-platonic commensurator quotient, by Proposition 3.9, whereas the latter does not (cf. Example 3.11).

The results of Sections 4 and 6 raise the following question:

Question 7.4 *For Λ equal to each of the $(2,3,6)$-, $(2,4,4)$-, and $(3,3,3)$-rotation groups, does there exist a one-cusped mixed-platonic orbifold with peripheral subgroup Λ? If so, what is the smallest-volume such example*?

Since the figure-8 knot complement and the dodecahedral knot complements are the only knot complements known to admit hidden symmetries and the only knot complements known to contain immersed closed totally geodesic surfaces, we can also ask:

Question 7.5 *Does every knot complement which admits hidden symmetries contain a closed, possibly immersed, totally geodesic surface*?

References

[1] **C C Adams**, *Noncompact hyperbolic 3-orbifolds of small volume*, from "Topology '90" (Columbus, OH, 1990) (B Apanasov, W D Neumann, A W Reid, L Siebenmann, editors), Ohio State Univ. Math. Res. Inst. Publ. 1, de Gruyter, Berlin (1992) 1–15 MR

[2] **C C Adams**, *Waist size for cusps in hyperbolic 3-manifolds*, Topology 41:2 (2002) 257–270 MR

[3] **I Agol**, *Bounds on exceptional Dehn filling*, Geom. Topol. 4 (2000) 431–449 MR

[4] **I R Aitchison**, **J H Rubinstein**, *Combinatorial cubings, cusps, and the dodecahedral knots*, from "Topology '90" (Columbus, OH, 1990) (B Apanasov, W D Neumann, A W Reid, L Siebenmann, editors), Ohio State Univ. Math. Res. Inst. Publ. 1, de Gruyter, Berlin (1992) 17–26 MR

[5] **B A Burton**, *The Pachner graph and the simplification of 3-sphere triangulations*, from "Computational geometry (SCG'11)", ACM, New York (2011) 153–162 MR

[6] **A Champanerkar**, **I Kofman**, **J S Purcell**, *Geometry of biperiodic alternating links*, J. Lond. Math. Soc. 99:3 (2019) 807–830 MR

[7] **D Chavey**, *Periodic tilings and tilings by regular polygons, I: Bounds on the number of orbits of vertices, edges and tiles*, Mitt. Math. Sem. Giessen 164 (1984) 37–50 MR

[8] **D Chavey**, *Tilings by regular polygons, III: Dodecagon-dense tilings*, Symmetry Cult. Sci. 25:3 (2014) 193–210

[9] **E Chesebro**, **M Chu**, **J DeBlois**, **N R Hoffman**, **P Mondal**, **G S Walsh**, *Mixed-platonic 3-manifolds*, preprint (2024) arXiv 2407.01708 See ancillary files available at https://arxiv.org/src/2407.01708v2/anc/MixedPlatonicSearch.py

[10] **E Chesebro**, **J DeBlois**, *Algebraic invariants, mutation, and commensurability of link complements*, Pacific J. Math. 267:2 (2014) 341–398 MR

[11] **D Coulson**, **O A Goodman**, **C D Hodgson**, **W D Neumann**, *Computing arithmetic invariants of 3-manifolds*, Experiment. Math. 9:1 (2000) 127–152 MR

[12] **M Culler**, **N M Dunfield**, **M Goerner**, **J R Weeks**, *SnapPy, a computer program for studying the geometry and topology of 3-manifolds* Available at http://snappy.computop.org

[13] **D B A Epstein**, **R C Penner**, *Euclidean decompositions of noncompact hyperbolic manifolds*, J. Differential Geom. 27:1 (1988) 67–80 MR

[14] **M Goerner**, *A census of hyperbolic platonic manifolds and augmented knotted trivalent graphs*, New York J. Math. 23 (2017) 527–553 MR

[15] **O Goodman**, **D Heard**, **C Hodgson**, *Commensurators of cusped hyperbolic manifolds*, Experiment. Math. 17:3 (2008) 283–306 MR

[16] **B Grünbaum**, **G C Shephard**, *Tilings and patterns*, W H Freeman and Company, New York (1987) MR

[17] **A Hatcher**, *Hyperbolic structures of arithmetic type on some link complements*, J. London Math. Soc. 27:2 (1983) 345–355 MR

[18] **N R Hoffman**, *On knot complements that decompose into regular ideal dodecahedra*, Geom. Dedicata 173 (2014) 299–308 MR

[19] **N R Hoffman**, *Small knot complements, exceptional surgeries and hidden symmetries*, Algebr. Geom. Topol. 14:6 (2014) 3227–3258 MR

[20] **N R Hoffman**, *Cusp types of quotients of hyperbolic knot complements*, Proc. Amer. Math. Soc. Ser. B 9 (2022) 336–350 MR

[21] **R Kirby**, *Problems in low-dimensional topology*, from "Geometric topology" (W H Kazez, editor), AMS/IP Stud. Adv. Math. 2.2, Amer. Math. Soc., Providence, RI (1997) 35–473 MR

[22] **O Krötenheerdt**, *Die homogenen Mosaike n-ter Ordnung in der euklidischen Ebene*, *I*, Wiss. Z. Martin-Luther-Univ. Halle-Wittenberg Math.-Natur. Reihe 18 (1969) 273–290 MR

[23] **M Lackenby**, *Word hyperbolic Dehn surgery*, Invent. Math. 140:2 (2000) 243–282 MR

[24] **C Maclachlan**, **A W Reid**, *The arithmetic of hyperbolic 3-manifolds*, Graduate Texts in Mathematics 219, Springer (2003) MR

[25] **D A Marcus**, *Number fields*, 2nd edition, Springer (2018) MR

[26] **R Meyerhoff**, *Sphere-packing and volume in hyperbolic 3-space*, Comment. Math. Helv. 61:2 (1986) 271–278 MR

[27] **W D Neumann**, **A W Reid**, *Arithmetic of hyperbolic manifolds*, from "Topology '90" (Columbus, OH, 1990) (B Apanasov, W D Neumann, A W Reid, L Siebenmann, editors), Ohio State Univ. Math. Res. Inst. Publ. 1, de Gruyter, Berlin (1992) 273–310 MR

[28] **W D Neumann**, **A W Reid**, *Notes on Adams' small volume orbifolds*, from "Topology '90" (Columbus, OH, 1990) (B Apanasov, W D Neumann, A W Reid, L Siebenmann, editors), Ohio State Univ. Math. Res. Inst. Publ. 1, de Gruyter, Berlin (1992) 311–314 MR

[29] **J G Ratcliffe**, *Foundations of hyperbolic manifolds*, 3rd edition, Graduate Texts in Mathematics 149, Springer (2019) MR

[30] **A W Reid**, *Arithmeticity of knot complements*, J. London Math. Soc. 43:1 (1991) 171–184 MR

[31] **A W Reid**, **G S Walsh**, *Commensurability classes of 2-bridge knot complements*, Algebr. Geom. Topol. 8:2 (2008) 1031–1057 MR

[32] *SageMath, version 10.0* (2023) Available at https://www.sagemath.org

[33] **W P Thurston**, *The geometry and topology of three-manifolds*, lecture notes, Princeton University (1979) Available at https://url.msp.org/gt3m

[34] **W P Thurston**, *Three-dimensional geometry and topology*, *I*, Princeton Mathematical Series 35, Princeton Univ. Press (1997) MR

ERIC CHESEBRO eric.chesebro@umt.edu
Department of Mathematical Sciences, University of Montana, Missoula, MT, United States

MICHELLE CHU mchu@umn.edu
School of Mathematics, University of Minnesota, Minneapolis, MN, United States

JASON DEBLOIS jdeblois@pitt.edu
Department of Mathematics, University of Pittsburgh, Pittsburgh, PA, United States

NEIL R HOFFMAN neilhoff@d.umn.edu
Swenson College of Science and Engineering, University of Minnesota Duluth, Duluth, MN, United States

PRIYADIP MONDAL priyadip@post.bgu.ac.il
Department of Mathematics, Ben Gurion University of the Negev, Be'er Sheva, Israel

GENEVIEVE S WALSH genevieve.walsh@tufts.edu
Department of Mathematics, Tufts University, Medford, MA, United States

Received: July 12, 2024 Revised: March 19, 2025

ALGEBRAIC & GEOMETRIC TOPOLOGY

msp.org/agt

EDITORS

PRINCIPAL ACADEMIC EDITORS

John Etnyre
etnyre@math.gatech.edu
Georgia Institute of Technology

Vesna Stojanoska
vesna@illinois.edu
University of Illinois at Urbana-Champaign

BOARD OF EDITORS

Julie Bergner	University of Virginia jeb2md@eservices.virginia.edu	Daniel Isaksen	Wayne State University isaksen@math.wayne.edu
Steven Boyer	Université du Québec à Montréal boyer.steven@uqam.ca	Thomas Koberda	University of Virginia thomas.koberda@virginia.edu
Tara E Brendle	University of Glasgow tara.brendle@glasgow.ac.uk	Markus Land	JGU Mainz mland@uni-mainz.de
Indira Chatterji	CNRS & Univ. Côte d'Azur (Nice) indira.chatterji@math.cnrs.fr	Christine Lescop	Université Joseph Fourier lescop@ujf-grenoble.fr
Octav Cornea	Université de Montreal cornea@dms.umontreal.ca	Norihiko Minami	OCAMI (Osaka Central Adv. Math. Inst.) norihikominami@gmail.com
Alexander Dranishnikov	University of Florida dranish@math.ufl.edu	Andrés Navas	Universidad de Santiago de Chile andres.navas@usach.cl
Tobias Ekholm	Uppsala University, Sweden tobias.ekholm@math.uu.se	Jessica S Purcell	Monash University jessica.purcell@monash.edu
Mario Eudave-Muñoz	Univ. Nacional Autónoma de México mario@matem.unam.mx	Birgit Richter	Universität Hamburg birgit.richter@uni-hamburg.de
David Futer	Temple University dfuter@temple.edu	Jérôme Scherer	École Polytech. Féd. de Lausanne jerome.scherer@epfl.ch
John Greenlees	University of Warwick john.greenlees@warwick.ac.uk	Zoltán Szabó	Princeton University szabo@math.princeton.edu
Matthew Hedden	Michigan State University mhedden@math.msu.edu	Maggy Tomova	University of Iowa maggy-tomova@uiowa.edu
Kristen Hendricks	Rutgers University kristen.hendricks@rutgers.edu	Daniel T Wise	McGill University, Canada daniel.wise@mcgill.ca
Hans-Werner Henn	Université Louis Pasteur henn@math.u-strasbg.fr	Lior Yanovski	Hebrew University of Jerusalem lior.yanovski@gmail.com
Kathryn Hess	École Polytechnique Féd. de Lausanne kathryn.hess@epfl.ch		

See inside back cover or msp.org/agt for submission instructions.

The subscription price for 2026 is US $795/year for the electronic version, and $1170/year (+$80, if shipping outside the US) for print and electronic. Subscriptions, requests for back issues and changes of subscriber address should be sent to MSP. Algebraic & Geometric Topology is indexed by Mathematical Reviews, Zentralblatt MATH, Current Mathematical Publications and the Science Citation Index.

Algebraic & Geometric Topology (ISSN 1472-2747 printed, 1472-2739 electronic) is published 9 times per year and continuously online, by Mathematical Sciences Publishers, 2000 Allston Way # 59, Berkeley, CA 94701-4004. Periodical rate postage paid at Oakland, CA 94615-9651, and additional mailing offices. POSTMASTER: send address changes to Mathematical Sciences Publishers, 2000 Allston Way # 59, Berkeley, CA 94701-4004.

AGT peer review and production are managed by EditFlow® from MSP.

PUBLISHED BY

mathematical sciences publishers

nonprofit scientific publishing

https://msp.org/

© 2026 Mathematical Sciences Publishers

ALGEBRAIC & GEOMETRIC TOPOLOGY

Volume 26 Issue 6 (pages 1965–2352) 2026

Detecting right-veering diffeomorphisms 1965
MIGUEL ORBEGOZO RODRÍGUEZ

A structural approach to tree decompositions of knots and spatial graphs 2015
CORENTIN LUNEL and ARNAUD DE MESMAY

Punctured JSJ tori and tautological extensions of Azumaya algebras 2049
YI WANG

Combination theorems for geometrically finite convergence groups 2079
ALEC TRAASETH and THEODORE WEISMAN

Modular links: bunch algorithm and upper volume bounds 2123
CONNIE ON YU HUI and JOSÉ ANDRÉS RODRÍGUEZ MIGUELES

Low complexity among principal fully irreducible elements of $\mathrm{Out}(F_3)$ 2157
NAOMI ANDREW, PAIGE HILLEN, ROBERT ALONZO LYMAN and CATHERINE EVA PFAFF

Dirichlet–Voronoi domain and injectivity radius of flag manifolds — equivariant cell structure on $O(3)/O(1)^3$ 2181
ARTHUR GARNIER

Mixed-platonic 3-manifolds 2215
ERIC CHESEBRO, MICHELLE CHU, JASON DEBLOIS, NEIL R HOFFMAN, PRIYADIP MONDAL and GENEVIEVE S WALSH

3d quantum trace map 2255
SAMUEL PANITCH and SUNGHYUK PARK

On the complexity of 2-bridge link complements 2315
JAMES MORGAN and JONATHAN SPREER